CHAOTIC VIBRATIONS OF THE ONE-DIMENSIONAL WAVE EQUATION DUE TO A SELF-EXCITATION BOUNDARY CONDITION. II. ENERGY INJECTION, PERIOD DOUBLING AND HOMOCLINIC ORBITS

GOONG CHEN[*]

Department of Mathematics, Texas A&M University,
College Station, Texas 77843, USA

SZE-BI HSU[†]

Department of Mathematics, National Tsing Hua University,
Hsinchu 30043, Taiwan, R.O.C.

JIANXIN ZHOU[‡]

Department of Mathematics, Texas A&M University,
College Station, Texas 77843, USA

Consider the initial-boundary value problem of the linear wave equation $w_{tt} - w_{xx} = 0$ on an interval. The boundary condition at the left endpoint is linear homogeneous, injecting energy into the system, while the boundary condition at the right endpoint has cubic nonlinearity of a van der Pol type. We show that the interactions of these linear and nonlinear boundary conditions can cause chaos to the Riemann invariants (u, v) of the wave equation when the parameters enter a certain regime. Period-doubling routes to chaos and homoclinic orbits are established. We further show that when the initial data are smooth satisfying certain compatibility conditions at the boundary points, the space-time trajectory or the state of the wave equation, which satisfies another type of the van der Pol boundary condition, can be chaotic. Numerical simulations are also illustrated.

1. Introduction

We continue the study from Part I [Chen *et al.*, 1998a] about chaotic vibrations of the one-dimensional wave equation due to a van der Pol type boundary condition by identifying some other sources causing chaos and by analyzing routes to chaos. In this paper, we focus on the interaction of this self-excitation nonlinear boundary condition at the right end $x = 1$ of the spatial span $x \in [0, 1]$ with a linear boundary condition injecting energy at the left end $x = 0$. The injection of energy, or *energy pumping*, brings instability into the vibrating system and excites otherwise (asymptotically) periodic motions into chaos. Two period-doubling routes to chaos can be confirmed. There also exist homoclinic orbits and homoclinic bifurcations. Unlike the models we have treated in Part I [Chen *et al.*, 1998a] and the sequel Part III [Chen *et al.*,

---

[*]E-mail: gchen@math.tamu.edu
[†]E-mail: sbhsu@am.nthu.edu.tw
[‡]E-mail: jzhou@math.tamu.edu

1998b] where issues of multiplicity (i.e. nonunique-ness) of solutions must be dealt with first, the PDE system we treat here has global *uniqueness* of solutions. Such solutions may even be C^∞-smooth on the space-time domain, allowing us to differentiate them and then to obtain other further conclusions (whereas those systems in Parts I and III [Chen *et al.*, 1998a, 1998b] definitely do not have globally C^1 solutions because the relevant interval maps are inherently discontinuous).

We proceed to describe the PDE system under study here. Let $w(x, t)$ satisfy the wave equation

$$w_{tt}(x, t) - w_{xx}(x, t) = 0, \qquad 0 < x < 1, \quad t > 0, \tag{1}$$

with a nonlinear self-excitation boundary condition at the right end $x = 1$:

$$w_x(1, t) = \alpha w_t(1, t) - \beta w_t^3(1, t), \\ 0 < \alpha \le 1, \quad \beta > 0, \tag{2}$$

and a linear boundary condition at the left end $x = 0$:

$$w_t(0, t) = -\eta w_x(0, t), \quad \eta > 0, \ \eta \neq 1, \ t > 0. \tag{3}$$

The remaining two conditions we require are the initial conditions

$$w(x, 0) = w_0(x), \ w_t(x, 0) = w_1(x), \quad x \in [0, 1]. \tag{4}$$

What is new here is the boundary condition (3). First, if it were true that $\eta = 0$ in (3), then $w_t(0, t) = 0$, for all $t > 0$; this is an energy-conserving boundary condition already treated by us in Part I [Chen *et al.*, 1998a, Sec. 3.1]. We showed that the Riemann invariants

$$u(x, t) = \frac{1}{2}[w_x(x, t) + w_t(x, t)], \\ v(x, t) = \frac{1}{2}[w_x(x, t) - w_t(x, t)], \tag{5}$$

of (1) are uniquely solvable and asymptotically time-periodic with period-2 for $0 < \alpha \le 1$, $\beta > 0$. What happens if $\eta \gtrless 0$? We may examine the rate

of change of energy of vibration:

$$\frac{d}{dt}E(t) = \frac{d}{dt}\left\{\frac{1}{2}\int_0^1 [w_x(x, t)^2 + w_t(x, t)^2]dx\right\} \\ = \eta w_x(0, t)^2 + w_t(1, t)^2[\alpha - \beta w_t(1, t)^2]. \tag{6}$$

We see that if $\eta > 0$ in (3), energy is added to the system from the left boundary point $x = 0$. The sign of η is "wrong" in the sense that it is opposite to the usual *impedance boundary condition* (cf. [Chen & Zhou, 1993, p. 24]) wherein η, signi-fying the damping coefficient, takes negative values. From now on, we call (3) an *energy injecting* boundary condition. Actually, using the method wave propagation ([Chen & Zhou, 1993, Sec. 1.6]) it is easy to show that the wave equation (1) subject to the *linear* boundary conditions

$$w_t(0, t) = -\eta w_x(0, t), \quad (\eta > 0, \ \eta \neq 1), \\ w_x(1, t) = 0, \quad t > 0,$$

and with initial conditions (4) has an *exponential energy growth rate*:

$$E(t) = \mathcal{O}(e^{kt}), \quad k = \ln\left(\left|\frac{1 + \eta}{1 - \eta}\right|\right) > 0, \\ \text{for } t > 0 \text{ large}. \tag{7}$$

This is commonly referred to as *instability* in the linear theory of differential equations. What can this linear instability do to the nonlinear self-excitation boundary condition (2)? As we will see, it will excite otherwise periodic vibrations into chaotic vibrations when η enters a certain regime. This also suggests that linear instability can make a non-chaotic nonlinear system chaotic, an idea which may prove useful in the recently emerged interests of *anticontrol*; see [Chen & Lai, 1997] and the references therein.

On the other hand, one may also pose the following question from the stabilization and control point of view: Given a distributed parameter vi-brating system with a linear unstable boundary condition such as (3) at the left end, can we de-sign a self-excitation boundary condition (2) to *regulate* the instability of the system? Our answer here is a qualified yes: Although instability still per-sists (cf. the unbounded sets U in Lemma 2.5), one can find bounded invariant intervals (the sets $\mathcal{I}$ in Lemma 2.5) on which the van der Pol type nonlin-earity can regulate linear instability to yield either asymptotically periodic or chaotic vibrations.

A reviewer of our paper has called our attention to some articles of pertinent interest: [Sharkovsky,

1994] and [Shimura, 1967]; see also the references therein. In those papers, a lossless transmission line terminated with a tunnel diode and a lumped parallel capacitor on one end, resulting in a nonlinear boundary condition, was discussed. The capacitor was then assumed degenerate to ensure mathematical tractability. The problems obviously have some flavor similar to ours. However, the nonlinearities under treatment and the methods used are quite different. Both those papers used the finite difference equation approach. Shimura [1967] showed the existence of some periodic solutions (but did not mention chaos), while the work of Sharkovsky [1994] does not seem to be self-contained. It appears, to the best of our knowledge, that we have achieved the most definitive conclusion and classification of chaotic vibration of the spatio-temporal nature.

Following Part I [Chen *et al.*, 1998a, (1.12), (1.13)] and using (5), we now convert (1) to an equivalent hyperbolic system

$$\frac{\partial}{\partial t}\begin{bmatrix} u(x,t) \\ v(x,t) \end{bmatrix} = \begin{bmatrix} 1 & 0 \\ 0 & -1 \end{bmatrix}\frac{\partial}{\partial x}\begin{bmatrix} u(x,t) \\ v(x,t) \end{bmatrix}, \quad (8)$$
$$0 < x < 1, \quad t > 0,$$

with boundary conditions

$$v(0,\,t) = G(u(0,\,t)) = G_\eta(u(0,\,t))$$
$$\equiv \frac{1+\eta}{1-\eta}u(0,\,t)\,, \quad t > 0\,, \quad (9)$$

$$u(1,\,t) = F(v(1,\,t))\,, \quad t > 0\,, \quad (10)$$

and initial conditions

$$u(x,\,0) \equiv u_0(x) = \frac{1}{2}[w_0'(x) + w_1(x)]\,,$$

$$v(x,\,0) \equiv v_0(x) = \frac{1}{2}[w_0'(x) - w_1(x)]\,, \quad (11)$$

$$0 \le x \le 1\,.$$

Note that in (10), $F = F_{\alpha,\beta}$, where $u = F_{\alpha,\beta}(v)$ is the *unique real* solution of the cubic equation

$$\beta(u-v)^3 + (1-\alpha)(u-v) + 2v = 0\,, \quad (12)$$
$$\beta > 0\,, \quad 0 < \alpha \le 1\,,$$

for each given v.

Using the method of characteristics, it is straightforward to show that the system (8)–(11) has a *unique* solution pair (u, v): for $t = 2k + \tau$, $k = 0, 1, 2, \ldots, 0 \le \tau < 2$, and $0 \le x \le 1$,

$$u(x,t) = \begin{cases} (F \circ G)^k(u_0(x+\tau))\,, & \tau \le 1 - x\,, \\ G^{-1} \circ (G \circ F)^{k+1}(v_0(2-x-\tau))\,, & 1-x < \tau \le 2-x\,, \\ (F \circ G)^{k+1}(u_0(\tau+x-2))\,, & 2-x < \tau \le 2\,; \end{cases} \quad (13)$$

$$v(x,\,t) = \begin{cases} (G \circ F)^k(v_0(x-\tau))\,, & \tau \le x\,, \\ G \circ (F \circ G)^k(u_0(\tau-x))\,, & x < \tau \le 1+x\,, \\ (G \circ F)^{k+1}(v_0(2+x-\tau))\,, & 1+x < \tau \le 2\,. \end{cases} \quad (14)$$

In the explicit representations above, $(F \circ G)^k$, e.g. means the kth iterate (composition) of the function $F \circ G$ with itself, a standard notation we have inherited from [Chen *et al.*, 1998]. (On the other hand, for a function $f(x)$, we use $f(x)^n$ to denote its nth power.) From (13) and (14), u and v are chaotic if $F \circ G$ and/or $G \circ F$ are chaotic.

In Sec. 2, we first provide quantitative information of important data such as derivatives, max and min, intercepts, etc., of the maps $F \circ G$ and $G \circ F$.

Section 3 studies the periodic-doubling routes to chaos. Here we show that $F \circ G$ and $G \circ F$ can be essentially treated as a *unimodal* [Devaney, 1989, p. 140] map as far as period-doubling bifurcations are concerned. However, we must emphasize that

$G \circ F$ is *not* equivalent to a unimodal map; see Remark 3.2. Two periodic-doubling bifurcation theorems are established: one for $0 < \eta < 1$ and the other for $\eta > 1$.

In Sec. 3, we show that homoclinic orbits and bifurcations exist for both $0 < \eta < 1$ and $\eta > 1$ on a bounded invariant interval.

When η is close to one, the instability becomes so strong that no bounded invariant intervals exist. In Sec. 4, we show that chaos can only exist on a Cantor-like repelling invariant set.

Differentiable solutions are shown to exist in Sec. 5. By differentiating such solutions, we show that the trajectory or state itself (rather than the

426   G. Chen et al.

gradient or the Riemann invariants) of (1)–(4) can become chaotic if another type of van der Pol condition (93) holds at $x = 1$.

Numerical simulations are also illustrated.

2. Preliminary Lemmas

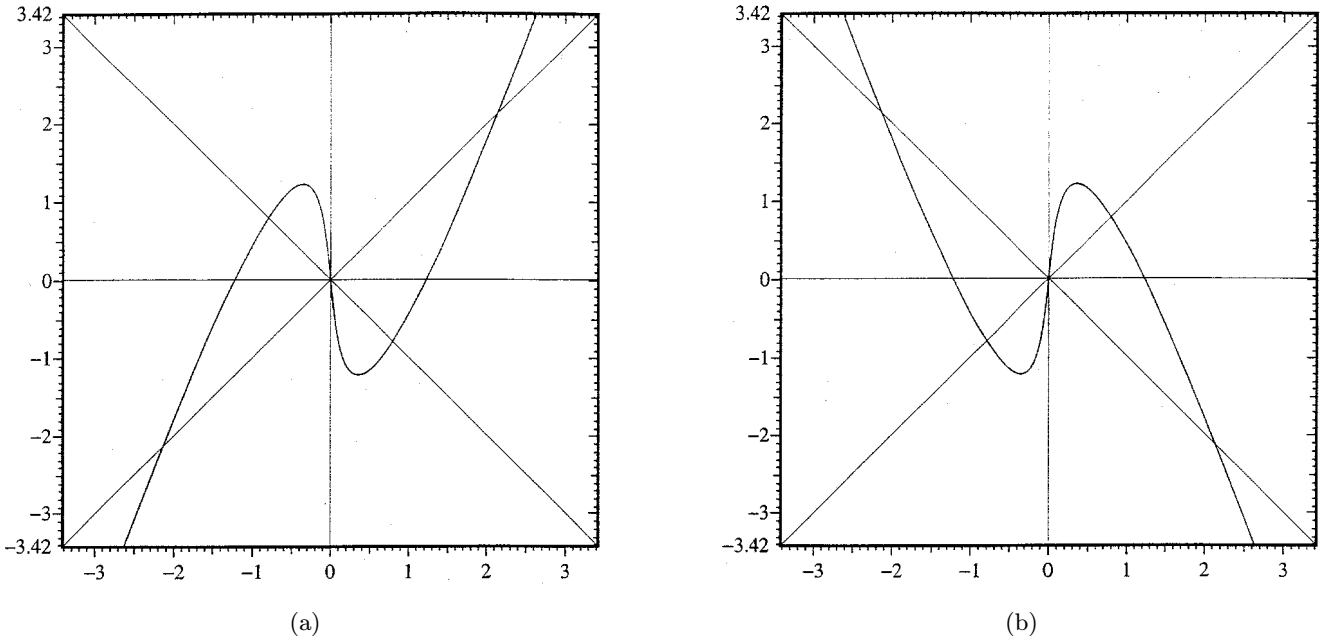As a visual aid for graphical analysis, we first display samples of the composite functions $G \circ F$ and

(a)

(b)

Fig. 1.   The graphs of $u = G \circ F(v) = G_\eta \circ F_{\alpha,\beta}(v)$, where $\alpha = 0.5$, $\beta = 1$ and (a) $\eta = 0.552$, (b) $\eta = 1.812$. It will be known later in Sec. 4 that these values of α, β and η make equalities hold in (66) and (67). Therefore homoclinic bifurcations occur; see Figs. 13 and 14 later.
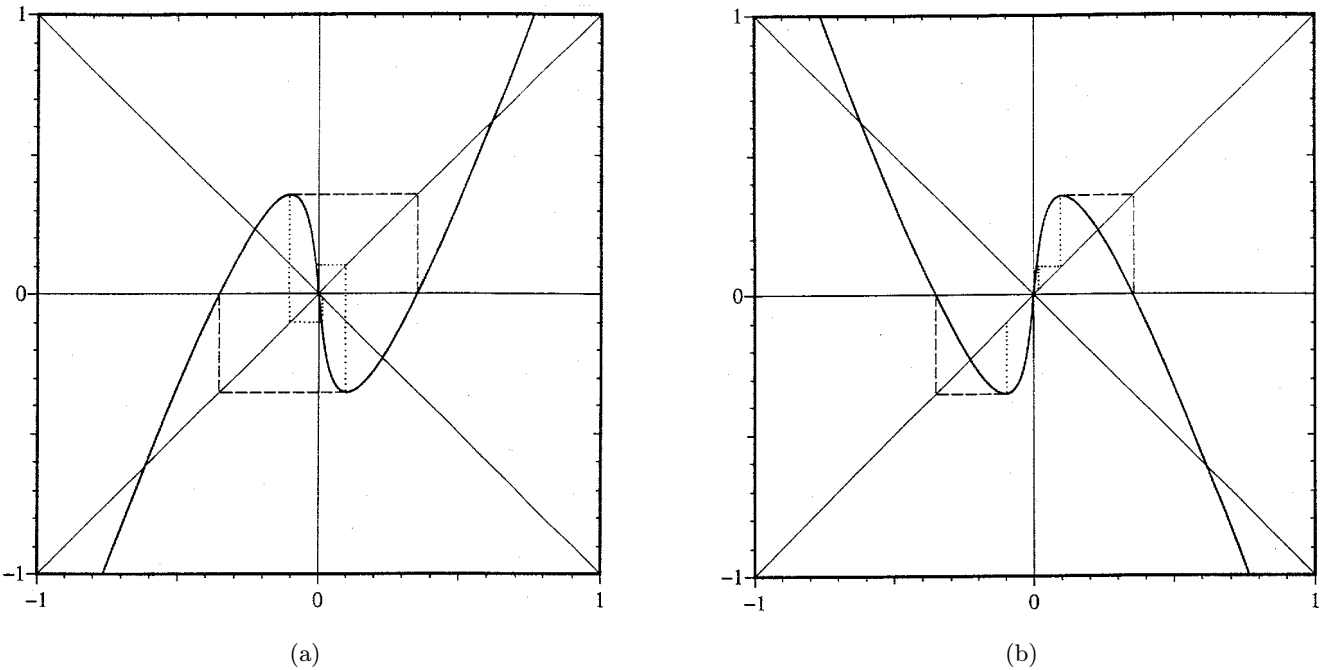

(a)

(b)

Fig. 2.   The graphs of $u = F \circ G(v) = F_{\alpha,\beta} \circ G_\eta(v)$, where $\alpha = 0.5$, $\beta = 1$ and (a) $\eta = 0.552$, (b) $\eta = 1.812$.

$F \circ G$ in Figs. 1 and 2. We next compile some useful properties of $G \circ F$ and $F \circ G$ in the following lemmas.

Lemma 2.1 (Derivative Formulas). *Let* $0 < \alpha \leq 1$, $\beta > 0$ *and* $\eta > 0$, $\eta \neq 1$, *where* α *and* β *are given and fixed, but* η *is a varying parameter. Define*

$$f_1(v, \eta) = G \circ F(v) = \frac{1 + \eta}{1 - \eta} F(v),$$

$$f_2(v, \eta) = F \circ G(v) = F\left(\frac{1 + \eta}{1 - \eta} v\right), \quad v \in \mathbb{R}. \tag{15}$$

Let $g(v)$ *be the unique real solution of the cubic equation*

$$\beta g(v)^3 + (1 - \alpha)g(v) + 2v = 0,$$
$$\text{for given} \quad v \in \mathbb{R}. \tag{16}$$

Then

$$\frac{\partial}{\partial v} f_1(v, \eta) = \frac{1 + \eta}{1 - \eta}\left[1 - \frac{2}{3\beta g(v)^2 + (1 - \alpha)}\right], \tag{17}$$

$$\frac{\partial}{\partial v} f_2(v, \eta) = \frac{1 + \eta}{1 - \eta}\left[1 - \frac{2}{3\beta g\left(\frac{1 + \eta}{1 - \eta} v\right)^2 + (1 - \alpha)}\right], \tag{18}$$

$$\frac{\partial}{\partial \eta} f_1(v, \eta) = \frac{2}{(1 - \eta)^2}[v + g(v)], \tag{19}$$

$$\frac{\partial}{\partial \eta} f_2(v, \eta) = \frac{2}{(1 - \eta)^2}\left[1 - \frac{2}{3\beta g\left(\frac{1 + \eta}{1 - \eta} v\right)^2 + (1 - \alpha)}\right], \tag{20}$$

$$\frac{\partial^2}{\partial \eta \partial v} f_1(v, \eta) = \frac{2}{(1 - \eta)^2}\left[1 - \frac{2}{3\beta g(v)^2 + (1 - \alpha)}\right], \tag{21}$$

$$\frac{\partial^2}{\partial \eta \partial v} f_2(v, \eta) = \frac{2}{(1 - \eta)^2}\left[1 - \frac{2}{3\beta g\left(\frac{1 + \eta}{1 - \eta} v\right)^2 + (1 - \alpha)} \right.$$
$$\left. - 24\beta\left(\frac{1 + \eta}{1 - \eta}\right)\frac{v \cdot g\left(\frac{1 + \eta}{1 - \eta} v\right)}{\left[3\beta g\left(\frac{1 + \eta}{1 - \eta} v\right)^2 + (1 - \alpha)\right]^3}\right], \tag{22}$$

$$\frac{\partial^2}{\partial v^2} f_1(v, \eta) = \frac{1 + \eta}{1 - \eta} \cdot (-24)\beta \cdot \frac{g(v)}{[3\beta g(v)^2 + (1 - \alpha)]^3}, \tag{23}$$

$$\frac{\partial^2}{\partial v^2} f_2(v, \eta) = \left(\frac{1 + \eta}{1 - \eta}\right)^2 (-24)\beta \cdot \frac{g\left(\frac{1 + \eta}{1 - \eta} v\right)}{\left[3\beta g\left(\frac{1 + \eta}{1 - \eta} v\right)^2 + (1 - \alpha)\right]^3}, \tag{24}$$

$$\frac{\partial^3}{\partial v^3} f_1(v, \eta) = \frac{1 + \eta}{1 - \eta} \cdot \frac{48\beta[-15\beta g(v)^2 + (1 - \alpha)]}{[3\beta g(v)^2 + (1 - \alpha)]^5}, \tag{25}$$

$$\frac{\partial^3}{\partial v^3} f_2(v, \eta) = \left(\frac{1+\eta}{1-\eta}\right)^3 \cdot \frac{48\beta \left[-15\beta g \left(\frac{1+\eta}{1-\eta}v\right)^2 + (1-\alpha)\right]}{\left[3\beta g \left(\frac{1+\eta}{1-\eta}v\right)^2 + (1-\alpha)\right]^5}.$$

(26)

Proof.   Straightforward verifications; cf. Part I [Chen *et al.*, 1998a, Sec. 3], for example.   ■

Lemma 2.2 (Intersections with the Lines $u - v = 0$ and $u + v = 0$).   *Let $\alpha: 0 < \alpha \leq 1$, $\beta > 0$, $\eta > 0$, $\eta \neq 1$, be given. Then*

(i) $u = G \circ F(v)$ *intersects the line $u = v$ at the points*

$$(u, v) = \left(-\frac{1+\eta}{2\eta}\sqrt{\frac{1+\alpha\eta}{\beta\eta}}, -\frac{1+\eta}{2\eta}\sqrt{\frac{1+\alpha\eta}{\beta\eta}}\right), (0, 0), \left(\frac{1+\eta}{2\eta}\sqrt{\frac{1+\alpha\eta}{\beta\eta}}, \frac{1+\eta}{2\eta}\sqrt{\frac{1+\alpha\eta}{\beta\eta}}\right);$$ (27)

(ii) $u = G \circ F(v)$ *intersects the line $u = -v$ at the points*

$$(u, v) = \left(-\frac{1+\eta}{2}\sqrt{\frac{\alpha+\eta}{\beta}}, \frac{1+\eta}{2}\sqrt{\frac{\alpha+\eta}{\beta}}\right), (0, 0), \left(\frac{1+\eta}{2}\sqrt{\frac{\alpha+\eta}{\beta}}, -\frac{1+\eta}{2}\sqrt{\frac{\alpha+\eta}{\beta}}\right);$$ (28)

(iii) $u = F \circ G(v)$ *intersects the line $u = v$ at the points*

$$(u, v) = \left(-\frac{1-\eta}{2\eta}\sqrt{\frac{1+\alpha\eta}{\beta\eta}}, -\frac{1-\eta}{2\eta}\sqrt{\frac{1+\alpha\eta}{\beta\eta}}\right), (0, 0), \left(\frac{1-\eta}{2\eta}\sqrt{\frac{1+\alpha\eta}{\beta\eta}}, \frac{1-\eta}{2\eta}\sqrt{\frac{1+\alpha\eta}{\beta\eta}}\right);$$ (29)

(iv) $u = F \circ G(v)$ *intersects the line $u = -v$ at the points*

$$(u, v) = \left(-\frac{1-\eta}{2}\sqrt{\frac{\alpha+\eta}{\beta}}, \frac{1-\eta}{2}\sqrt{\frac{\alpha+\eta}{\beta}}\right), (0, 0), \left(\frac{1-\eta}{2}\sqrt{\frac{\alpha+\eta}{\beta}}, -\frac{1-\eta}{2}\sqrt{\frac{\alpha+\eta}{\beta}}\right).$$ (30)

Proof.   We will verify only (i); (ii)–(iv) can be done in a similar way.

We solve $u = G \circ F(v) = v$ by taking the definition of G and F from (12), (15) and (16):

$$\frac{1+\eta}{1-\eta}[v + g(v)] = v,$$

$$g(v) + \frac{2\eta}{1+\eta}v = 0.$$

(31)

By (16),

$$\beta g(v)^3 + (1-\alpha)g(v) + 2v = 0,$$

$$\beta \left[\left(g(v) + \frac{2\eta}{1+\eta}v\right) - \frac{2\eta}{1+\eta}v\right]^3$$

$$+ (1-\alpha)\left[\left(g(v) + \frac{2\eta}{1+\eta}v\right) - \frac{2\eta}{1+\eta}v\right] + 2v = 0.$$

Using (31), we get

$$-\beta \left(\frac{2\eta}{1+\eta}v\right)^3 - (1-\alpha)\left(\frac{2\eta}{1+\eta}v\right) + 2v = 0.$$

Therefore

$$v = 0, \quad v = \pm\frac{1+\eta}{2\eta}\sqrt{\frac{1+\alpha\eta}{\beta\eta}},$$

and (27) has been verified.   ■

Lemma 2.3 (*v*-axis Intercepts).   *Let $\alpha: 0 < \alpha \leq 1$, $\beta > 0$, $\eta > 0$, $\eta \neq 1$, be given. Then*

(i) $u = G \circ F(v)$ *has v-axis intercepts*

$$v = -\sqrt{\frac{1+\alpha}{\beta}}, \ 0, \ \sqrt{\frac{1+\alpha}{\beta}};$$ (32)

(ii) $u = F \circ G(v)$ *has v-axis intercepts*

$$v = -\frac{1-\eta}{1+\eta}\sqrt{\frac{1+\alpha}{\beta}}, \; 0, \; \frac{1-\eta}{1+\eta}\sqrt{\frac{1+\alpha}{\beta}}. \quad (33)$$

Proof. Straightforward verifications. ∎

Lemma 2.4 (Local Maximum, Minimum and Piecewise Monotonicity). *Let $\alpha\colon 0 < \alpha \le 1$, $\beta > 0$, $\eta > 0$, $\eta \ne 1$, and α, β, η be fixed.*

(i) *If $0 < \eta < 1$, then $G \circ F$ has local extremal values*

$$M = G \circ F(-v_c) = \frac{1+\eta}{1-\eta}\frac{1+\alpha}{3}\sqrt{\frac{1+\alpha}{3\beta}}, \quad (34)$$

$$m = G \circ F(v_c) = -\frac{1+\eta}{1-\eta}\frac{1+\alpha}{3}\sqrt{\frac{1+\alpha}{3\beta}}, \quad (35)$$

where $v_c = [(2-\alpha)/3]\sqrt{(1+\alpha)/3\beta}$, and M, m are, respectively, the local maximum and minimum of $G \circ F$. The function $G \circ F$ is strictly increasing on $(-\infty, -v_c)$ and (v_c, ∞), but strictly decreasing on $(-v_c, v_c)$.

On the other hand, if $\eta > 1$, then $G \circ F$ has local minimum (m) and maximum (M) values

$$m = G \circ F(-v_c) = \frac{1+\eta}{1-\eta}\frac{1+\alpha}{3}\sqrt{\frac{1+\alpha}{3\beta}}, \quad (36)$$

$$M = G \circ F(v_c) = -\frac{1+\eta}{1-\eta}\frac{1+\alpha}{3}\sqrt{\frac{1+\alpha}{3\beta}}, \quad (37)$$

where v_c is the same as before. The function $G \circ F$ is strictly decreasing on $(-\infty, -v_c)$ and (v_c, ∞), but strictly increasing on $(-v_c, v_c)$.

(ii) *If $0 < \eta < 1$, then $F \circ G$ has local extremal values*

$$M = F \circ G(-\tilde{v}_c) = \frac{1+\alpha}{3}\sqrt{\frac{1+\alpha}{3\beta}}, \quad (38)$$

$$m = F \circ G(\tilde{v}_c) = -\frac{1+\alpha}{3}\sqrt{\frac{1+\alpha}{3\beta}}, \quad (39)$$

where $\tilde{v}_c = |(1-\eta)/(1+\eta)| \cdot [(2-\alpha)/3] \cdot \sqrt{(1+\alpha)/(3\beta)}$. The function $F \circ G$ is strictly increasing on $(-\infty, -\tilde{v}_c)$ and $(\tilde{v}_c, \infty)$, but strictly decreasing on $(-\tilde{v}_c, \tilde{v}_c)$.

On the other hand, if $\eta > 1$, then $F \circ G$ has local extremal values

$$m = F \circ G(-\tilde{v}_c) = -\frac{1+\alpha}{3}\sqrt{\frac{1+\alpha}{3\beta}},$$

$$M = F \circ G(\tilde{v}_c) = \frac{1+\alpha}{3}\sqrt{\frac{1+\alpha}{3\beta}}.$$

The function $F \circ G$ is strictly decreasing on $(-\infty, -\tilde{v}_c)$ and $(\tilde{v}_c, \infty)$, but strictly increasing on $(-\tilde{v}_c, \tilde{v}_c)$.

Proof. Use (17), etc., and carry out the computations. ∎

Lemma 2.5 (Bounded Invariant Intervals). *Let $0 < \alpha \le 1$, $\beta > 0$, and $\eta > 0$, $\eta \ne 1$.*

(i) *If $0 < \eta < 1$ and*

$$M = \frac{1+\eta}{1-\eta}\frac{1+\alpha}{3}\sqrt{\frac{1+\alpha}{3\beta}} \le \frac{1+\eta}{2\eta}\sqrt{\frac{1+\alpha\eta}{\beta\eta}}, \quad (40)$$

then the iterates of every point in the set $U \equiv (-\infty, -[(1+\eta)/2\eta]\sqrt{(1+\alpha\eta)/(\beta\eta)}) \cup ([(1+\eta)/2\eta]\sqrt{[(1+\alpha\eta)/\beta\eta]}, \infty)$ escape to $\pm\infty$, while those of any point in $\mathbb{R}\backslash\overline{U}$ are attracted to the bounded invariant interval $\mathcal{I} \equiv [-M, M]$ of $G \circ F$.

(ii) *If $\eta > 1$ and*

$$M = -\frac{1+\eta}{1-\eta}\frac{1+\alpha}{3}\sqrt{\frac{1+\alpha}{3\beta}} \le \frac{1+\eta}{2}\sqrt{\frac{\alpha+\eta}{\beta}}, \quad (41)$$

then the same conclusion as in (i) holds, with $U \equiv (-\infty, -[(1+\eta)/2]\sqrt{[(\alpha+\eta)/\beta]}) \cup ([(1+\eta)/2]\sqrt{(\alpha+\eta)/\beta}, \infty)$ and $\mathcal{I} \equiv [-M, M]$ for $G \circ F$.

(iii) *If $0 < \eta < 1$ and*

$$M = \frac{1+\alpha}{3}\sqrt{\frac{1+\alpha}{3\beta}} \le \frac{1-\eta}{2\eta}\sqrt{\frac{1+\alpha\eta}{\beta\eta}}, \quad (42)$$

then the same conclusion holds, with $U \equiv (-\infty, -[(1-\eta)/(2\eta)]\sqrt{(1+\alpha\eta)/(\beta\eta)}) \cup ([(1-\eta)/(2\eta)]\sqrt{[(1+\alpha\eta)/(\beta\eta)]}, \infty)$ and $\mathcal{I} \equiv [-M, M]$ for $F \circ G$.

(iv) *If $\eta > 1$ and*

$$M = \frac{1+\alpha}{3}\sqrt{\frac{1+\alpha}{3\beta}} \le -\frac{1-\eta}{2}\sqrt{\frac{\alpha+\eta}{\beta}}, \quad (43)$$

then the same conclusion holds, with $U \equiv (-\infty, -[(1 - \eta)/2]\sqrt{(\alpha + \eta)/\beta}) \cup ([(1 - \eta)/2]\sqrt{(\alpha + \eta)/\beta}, \infty)$ and $\mathcal{I} \equiv [-M, M]$ for $F \circ G$.

Proof. The results follow easily from Lemmas 2.2 and 2.4 and other piecewise monotonic properties of $G \circ F$ and $F \circ G$, as can be directly confirmed by graphical analysis from Figs. 1 and 2. We omit the details. ∎

Remark 2.1.

(i) Note that the two inequalities (40) and (42) are equivalent, so are (41) and (43).
(ii) We call the sets U in Lemma 2.5 the unstable sets, and the sets $\mathcal{I}$ the bounded stable sets.
(iii) When the condition (40) [equivalently, (41) or (42)] [equivalently, (43)] is violated, bounded invariant interval $\mathcal{I}$ no longer exists. Instead, we have a bounded Cantor-like invariant set; see Sec. 5.

3. Period-Doubling Routes to Chaos

We show that there are two period-doubling routes to chaos: one occurring during $\eta: 0 < \eta < 1$, and the other during $\eta > 1$.

We first consider the case $0 < \eta < 1$.

The maps $G \circ F$ and $F \circ G$, as displayed in Figs. 1(a) and 2(a), have a hump and a dip around $\pm v_c$, for the critical value v_c given in Lemma 2.4. Such profiles are definitely *not unimodal*. In the exploration of period-2^n points, $n = 1, 2, \ldots$, of $G \circ F$ and $F \circ G$ for varying $\eta: 0 < \eta < 1$ while α and β are held fixed, as it turns out, for all practical purposes $G \circ F$ and $F \circ G$ can be treated as unimodal maps. This is because of a simple correspondence of period-2^n orbits as given below in Lemma 3.1 obtained from the oddness of the maps $G \circ F$ and $F \circ G$.

Lemma 3.1 (Correspondence of Period-2^n Orbits to a Unimodal Map). *Let $0 < \alpha \leq 1$, $\beta > 0$ and $0 < \eta < 1$. Assume that α, β and η satisfy*

$$M = \frac{1 + \eta}{1 - \eta} \frac{1 + \alpha}{3} \sqrt{\frac{1 + \alpha}{3\beta}} \leq \sqrt{\frac{1 + \alpha}{\beta}}, \qquad (44)$$

where M is the local maximum value of $G \circ F = G_\eta \circ F_{\alpha,\beta}$ in (34), and $\sqrt{(1 + \alpha)/\beta}$ is the positive v-axis intercept of $G \circ F$ from Lemma 2.3. Assume that $x_0 \in [-M, M]$ is a periodic point of

prime period-2^n, for some $n \in \{2, 3, 4, \ldots\}$. Then $|x_0|$ is also a periodic point of $H = -G \circ F$ of prime period-2^n such that all the points on the orbit $\{H^j(|x_0|)|j = 0, 1, \ldots, 2^n - 1\}$ are positive.

Conversely, let $x_0 > 0$ be a periodic point of prime period-2^n of H for some $n \in \{2, 3, 4, \ldots\}$. Then $\{(-1)^j H^j(x_0)|j = 0, 1, \ldots, 2^n - 1\}$ is the full orbit of x_0 of the map $G \circ F$ of prime period 2^n.

The period-2^n orbit, $n \geq 2$, of $G \circ F$ is attracting (resp., repelling) if and only if the corresponding period-2^n orbit of H is attracting (resp., repelling). The same is true for $F \circ G$.

Proof. The map $G \circ F$ is an odd function such that

$$\begin{aligned} G \circ F(x) > 0 \quad &\text{if } x < 0, \\ G \circ F(x) < 0 \quad &\text{if } x > 0, \\ \text{for } x \in \left[-\sqrt{\frac{1 + \alpha}{\beta}}, \sqrt{\frac{1 + \alpha}{\beta}} \right]. & \end{aligned} \qquad (45)$$

Since $0 < \eta < 1$, we have $\sqrt{(1 + \alpha)/\beta} \leq [(1 + \eta) \cdot (1 + \alpha\eta)^{1/2}]/[2\eta \cdot (\beta\eta)^{1/2}]$; Lemma 2.5 (i) and Eq. (19) are applicable on the invariant interval $[-M, M]$ of $G \circ F$. Let x_0 be a period-2^n point of $G \circ F$. Then $x_0 \in [-M, M]$, and its full orbit forms a sequence with alternating signs:

$$x_0, x_1, x_2, \ldots, x_{2^n - 1}, \quad \text{where} \quad x_j = (G \circ F)^j x_0. \qquad (46)$$

Without loss of generality, we may assume that $x_0 > 0$. Obviously,

$$\{(-1)^j x_j | j = 0, 1, \ldots, 2^n - 1\} \qquad (47)$$

forms a period-2^n orbit of H such that $(-1)^j x_j = |x_j| = H^j(x_0) > 0$, $j = 0, 1, \ldots, 2^n - 1$. We now verify that (46) is also an orbit of *prime period-2^n* of H. It is easy to see that if all the elements in the set $\{|x_j| | j = 0, 1, \ldots, 2^n - 1\}$ are distinct, then because $H = -G \circ F$, (46) is a full orbit of prime period-2^n of H. Consider the remaining possibility that elements in (46) are not distinct. Without loss of generality, we may assume that j_0 is the smallest positive index such that

$$x_0 = (-1)^{j_0} x_{j_0}, \quad \text{for some } j_0 \in \{1, 2, \ldots, 2^n - 1\}. \qquad (48)$$

Since $x_0 > 0$ and $x_{j_0} = (-1)^{j_0}|x_{j_0}|$ by (45) and (46), we see that (48) holds if and only if $j_0 =$

odd $= 2k + 1$ for some nonnegative integer k, and $|x_{j_0}| = x_0$. Therefore the sequence (46) becomes

$$x_0, x_1, \ldots, x_{j_0-1}, x_{j_0} = -x_0, -x_1, -x_2, \ldots,$$
$$-x_{j_0-1}, -x_{j_0} = x_0.$$

This gives

$$x_0 = (G \circ F)^{2j_0}(x_0) = (G \circ F)^{2(2k+1)}(x_0)$$
$$= (G \circ F)^{2^n}(x_0). \tag{49}$$

Since x_0 is of prime period-2^n for the map $G \circ F$, we get

$$2(2k+1) = 2^n.$$

This is possible if and only if $k = 0$, or $n = 1$. If $n > 1$, the above will lead to a contradiction. Therefore if $n \in \{2, 3, 4, \ldots\}$, then any prime period-$2^n$ orbit (46) of $G \circ F$ will have a corresponding prime period-2^n orbit (44) of H.

Conversely, let $\{y_0, y_1, \ldots, y_{2^n-1}\}$ be a prime period-2^n orbit of H. Then this orbit consists of distinct members. It is easy to see that the set $\{y_0, -y_1, y_2, -y_3, \ldots, -y_{2^n-1}\}$ is also distinct, and therefore it is a full prime period-2^n orbit of $G \circ F$.

The attracting or repelling property of the period-2^n orbit (46) of $G \circ F$ implies (and is implied by) that of the period-2^n orbit (47) of H because of the simple fact that $G \circ F$ is an odd function.

The proof for $F \circ G$ is similar under the same condition (44). ∎

Remark 3.1. Lemma 3.1 does not hold for $n = 1$. When $n = 1$, by (28), $G \circ F$ has a prime period-2 orbit $\{-[(1 + \eta)/2]\sqrt{(\alpha + \beta)/\beta},\ [(1 + \eta)/2]\sqrt{(\alpha + \eta)/\beta}\}$, while the corresponding orbit of H has period-1: $\{[(1 + \eta)/2]\sqrt{(\alpha + \eta)/\beta}\}$.

Define

$$\underline{\eta}_H = \underline{\eta}_H(\alpha) = \left(1 - \frac{1+\alpha}{3\sqrt{3}}\right) \Big/ \left(1 + \frac{1+\alpha}{3\sqrt{3}}\right). \tag{50}$$

Then $0 < \underline{\eta}_H < 1$ and (44) holds if and only if $0 < \eta \le \underline{\eta}_H$. (The parameter value $\underline{\eta}_H$ will be known in Theorem 4.1 in Sec. 4 to be related to *degenerate homoclinic orbits*.) For such η, the map $H = -G \circ F$ (as well as $-F \circ G$) is unimodal on the interval $\tilde{I} \equiv [0, \sqrt{(1 + \alpha)/\beta}]$. We can apply the Period-Doubling Bifurcation Theorem to H on $\tilde{I}$ instead of to the non-unimodal $G \circ F$ on $(-\tilde{I}) \cup \tilde{I}$.

Theorem 3.1 (Period-Doubling Bifurcation Theorem for $H = -G \circ F$ on $\tilde{I}$, $0 < \eta < 1$). *Let*

$\alpha: 0 < \alpha \le 1$, $\beta > 0$ *be fixed, and let* $\eta: 0 < \eta \le \underline{\eta}_H$ *be a varying parameter. Let* $h_1(v, \eta) = -f_1(v, \eta) = -G \circ F(v)$, *cf. (15). Then*

(i) $v_0(\eta) = [(1 + \eta)/2]\sqrt{(\alpha + \eta)/\beta}$ *is a curve of fixed points of* $h_1: h_1(v_0(\eta), \eta) = v_0(\eta)$.

(ii) *The algebraic equation*

$$\frac{1}{2}\left(\frac{1+\alpha\eta}{3\beta\eta}\right)^{1/2}\left[\frac{1+(3-2\alpha)\eta}{3\eta}\right] = \frac{1+\eta}{2}\sqrt{\frac{\alpha+\eta}{\beta}} \tag{51}$$

has a unique solution $\eta = \eta_0: 0 < \eta_0 \le \underline{\eta}_H$, *for any given* $\alpha: 0 < \alpha \le 1$ *and* $\beta > 0$. *(Actually, η_0 is independent of β.) We have*

$$\frac{\partial}{\partial v}h_1(v, \eta)\Big|_{\substack{v=v_0(\eta_0)\\ \eta=\eta_0}} = -1. \tag{52}$$

(iii) *For* $\eta = \eta_0$ *satisfying (51), we have*

$$A \equiv \left[\frac{\partial^2 h_1}{\partial\eta\partial v} + \frac{1}{2}\left(\frac{\partial h_1}{\partial\eta}\right)\frac{\partial^2 h_1}{\partial v^2}\right]\Bigg|_{\substack{v=v_0(\eta_0)\\ \eta=\eta_0}}$$
$$= -\frac{[4\alpha(2\alpha+3)+6]\eta_0^3+(4\alpha+6)\eta_0^2-10\eta_0+6}{3(1-\eta_0)^3(1+\eta_0)^2}$$
$$\ne 0. \tag{53}$$

(iv) *For* η_0 *given in (ii), we have*

$$B \equiv \left[\frac{1}{6}\frac{\partial^3 h_1}{\partial v^3} + \frac{1}{4}\left(\frac{\partial^2 h_1}{\partial v^2}\right)^2\right]\Bigg|_{\substack{v=v_0(\eta_0)\\ \eta=\eta_0}}$$
$$= \frac{8\beta\eta_0^4\{(1-\eta_0)[(6\alpha-1)\eta_0+5]+6\eta_0(1+\alpha\eta_0)\}}{(1-\eta_0)^2(1+\eta_0)^4}$$
$$> 0. \tag{54}$$

Consequently, there is period-doubling bifurcation at $(v_0(\eta_0), \eta_0)$. *The stability type of the bifurcated period-2 orbit is attracting.*

Proof.

(i) This is an immediate consequence of Lemma 2.2 (ii).

(ii) We first determine the point(s) $v > 0$ such that $\partial h_1/\partial v = -1$. By (17), with a change of sign for f_1 therein, we get

$$-\frac{1+\eta}{1-\eta}\left[1 - \frac{2}{3\beta g(v)^2 + (1-\alpha)}\right] = -1.$$

Therefore

$$3\beta g(v)^2 + (1 - \alpha) = \frac{1+\eta}{\eta},$$

$$g(v) = \pm \left(\frac{1+\alpha\eta}{3\beta\eta}\right)^{1/2}. \tag{55}$$

We choose the "−" sign in (55) because otherwise, as the subsequent calculations would imply, v becomes negative which is outside $\tilde{I}$ and thus undesirable. Hence

$$g(v) = -\left(\frac{1+\alpha\eta}{3\beta\eta}\right)^{1/2}. \tag{56}$$

Since $g(v)$ satisfies (16), from (56) we get

$$v = -\frac{1}{2}[\beta g(v)^3 + (1-\alpha)g(v)]$$

$$= -\frac{1}{2}\left\{\beta\left[g(v) + \left(\frac{1+\alpha\eta}{3\beta\eta}\right)^{1/2}\right.\right.$$

$$\left. - \left(\frac{1+\alpha\eta}{3\beta\eta}\right)^{1/2}\right]^3 \tag{57}$$

$$+ (1-\alpha)\left[g(v) + \left(\frac{1+\alpha\eta}{3\beta\eta}\right)^{1/2}\right.$$

$$\left.\left. - \left(\frac{1+\alpha\eta}{3\beta\eta}\right)^{1/2}\right]\right\}$$

$$= \frac{1}{2}\left[\beta\left(\frac{1+\alpha\eta}{3\beta\eta}\right)^{3/2} + (1-\alpha)\left(\frac{1+\alpha\eta}{3\beta\eta}\right)^{1/2}\right]$$

$$= \text{LHS of (51)}. \tag{58}$$

Further setting (58) equal to $v_0(\eta)$ in (i), we get the RHS of (51).

To show that (51) has a unique solution $\eta_0 : 0 < \eta_0 \le \underline{\eta}_H$ for given α (as η_0 can be easily seen to be independent of β), only some elementary arguments (or direct computer verification) are needed. Since much of this is geometrically and visually obvious, it is quite unnecessary to provide the details.

(iii) We apply (17), (19) and (23) to obtain $\partial^2 f_1/\partial\eta\partial v$, $\partial f_1/\partial\eta$ and $\partial^2 f_1/\partial v^2$. Because $h_1 = -f_1$, we just need to adjust the signs to get $\partial^2 h_1/\partial\eta\partial v$, etc. Simplifying, and using

(56), we obtain

$$A \equiv \left[\frac{\partial^2 h_1}{\partial\eta\partial v} + \frac{1}{2}\left(\frac{\partial h_1}{\partial\eta}\right)\frac{\partial^2 h_1}{\partial v^2}\right]\Bigg|_{v=v_0(\eta),\eta=\eta_0}$$

$$= \frac{\{-6(1-\eta_0)^2(1+\eta_0)-[(3+2\alpha)\eta_0-1]}{\cdot(4\alpha\eta_0^2+4\eta_0)\}}{3(1-\eta_0)^3(1+\eta_0)^2}$$

$$= (53).$$

To show that $A \ne 0$, one can use a computer-assisted proof by plotting the graph of η versus α for the real points η making $A = 0$:

$$[4\alpha(3+2\alpha)+6]\eta^3 + (4\alpha+6)\eta^2 - 10\eta + 6 = 0$$

Our numerical work has shown that for $\alpha \in [0, 1]$, η is a monotonically increasing function with minimum ≈ -2.0506 and maximum $= -1$. Therefore $A \ne 0$ for $\eta_0 \in [0, 1)$.

(iv) B can be obtained similarly as in part (iii). Since $0 < \eta_0 < 1$, it is easy to see that $B > 0$.

We can now quote the Period-Doubling Bifurcation Theorem (see [Chow & Hale, 1982; Robinson, 1995, p. 220]) to conclude the proof. ∎

We now consider the period-doubling of $G \circ F$ for $\eta > 1$. Define

$$\overline{\eta}_H = \overline{\eta}_H(\alpha) = \left(1 + \frac{1+\alpha}{3\sqrt{3}}\right)\left(1 - \frac{1+\alpha}{3\sqrt{3}}\right)^{-1}. \tag{59}$$

Then $\overline{\eta}_H > 1$. This parameter value $\overline{\eta}_H$ will also be related to degenerate homoclinic orbits in Sec. 4; see Theorem 4.2. Then $\eta \in [\overline{\eta}_H, \infty)$ if and only if

$$0 < M \equiv -\frac{1+\eta}{1-\eta}\frac{1+\alpha}{3}\sqrt{\frac{1+\alpha}{3\beta}} \le \sqrt{\frac{1+\alpha}{\beta}},$$

where M comes from (41). For $\eta \in [\overline{\eta}_H, \infty)$, the map $G \circ F$ is unimodal on $\tilde{I} \equiv [0, \sqrt{(1+\alpha)/\beta}]$ and $-\tilde{I}$, separately. Period-2^n orbits of $G \circ F$ will exist on $\tilde{I}$ and $-\tilde{I}$ separately, and thus extra work such as Lemma 3.1 will no longer be needed.

Theorem 3.2 (Period-Doubling Bifurcation Theorem for $G \circ F$ on $\tilde{I}$, $\eta > 1$). *Let $\alpha : 0 < \alpha \le 1$, $\beta > 0$ be fixed, and let $\eta \in (\overline{\eta}_H, \infty)$ be a varying parameter. Let $f_1(v, \eta)$ be given as in (15). Then*

(i) *$v_0(\eta) = [(1+\eta)/2\eta]\sqrt{(1+\alpha\eta)/\beta\eta}$ is a curve of fixed points of $f_1 : f_1(v_0(\eta), \eta) = v_0(\eta)$.*

(ii) *The algebraic equation*

$$\frac{1}{6}\left(\frac{\alpha+\eta}{3\beta}\right)^{1/2}(3+\eta-2\alpha)=\frac{1+\eta}{2\eta}\sqrt{\frac{1+\alpha\eta}{\beta\eta}}$$

$$(60)$$

has a unique solution $\eta=\eta_0$: $\overline{\eta}_H\le\eta_0<\infty$ *for any given* α: $0<\alpha\le 1$ *and* $\beta>0$. (*Actually*, η_0 *is independent of* β.) *We have*

$$\frac{\partial}{\partial v}f_1(v,\,\eta)\Big|_{\substack{v=v_0(\eta_0)\\\eta=\eta_0}}=-1\,.$$

(iii) *For* $\eta=\eta_0$ *satisfying* (*60*), *we have*

$$A\equiv\left[\frac{\partial^2 f_1}{\partial\eta\partial v}+\frac{1}{2}\left(\frac{\partial f_1}{\partial\eta}\right)\left(\frac{\partial^2 f_1}{\partial v^2}\right)\right]\Bigg|_{\substack{v=v_0(\eta_0)\\\eta=\eta_0}}$$

$$=-\frac{6\eta_0^3-10\eta_0^2+(4\alpha+6)\eta_0+[4\alpha(2\alpha+3)+6]}{3(1-\eta_0)^3(1+\eta_0)^2}$$

$$\ne 0\,.$$

(iv) *For* η_0 *given in* (*ii*), *we have*

$$B\equiv\left[\frac{1}{6}\frac{\partial^3 f_1}{\partial v^3}+\frac{1}{4}\left(\frac{\partial^2 f_1}{\partial v^2}\right)^2\right]\Bigg|_{\substack{v=v_0(\eta_0)\\\eta=\eta_0}}$$

$$=\frac{8\beta\{(\eta_0-1)[5\eta_0-(6\alpha-1)]+6(\alpha+\eta_0)\}}{(1-\eta_0)^2(1+\eta_0)^4}$$

$$>0\,.$$

Consequently, there is period-doubling bifurcation at $(v_0(\eta_0),\,\eta_0)$. *The stability type of the bifurcated period-2 orbit is attracting.*

Proof. Similar to that of Theorem 3.1. ∎

By Theorems 3.1 and 3.2, and the unimodal properties of the maps involved, it is now obvious that a renormalization procedure as indicated by Feigenbaum [1978] and Collet and Tresser [1978] can be applied. Therefore the map $G\circ F=G_\eta\circ F_{\alpha,\beta}$ undergoes two period-doubling routes to chaos: one for $\eta\in(0,\,\underline{\eta}_H]$ and the other for $\eta\in[\overline{\eta}_H,\,\infty)$. After the completion of period-doubling, therefore, u and v become chaotic.

Similar Period-Doubling Bifurcation Theorems for the map $F\circ G$ for the cases $0<\eta<1$ and $\eta>1$ can be established as Theorems 3.1 and 3.2. However, the calculations of the constants A and B

[cf. (53) and (54)] are somewhat more involved and quite cumbersome as well. As it turns out, such work is unnecessary, because $F\circ G$ and $G\circ F$ are topologically conjugate, as the following commutative diagram shows:

$$\begin{array}{ccc}\mathbb{R} & \xrightarrow{G_\eta\circ F_{\alpha,\beta}} & \mathbb{R}\\ G_\eta^{-1}\downarrow & & \downarrow G_\eta^{-1}\\ \mathbb{R} & \xrightarrow{F_{\alpha,\beta}\circ G_\eta} & \mathbb{R}\end{array}$$

Therefore the period-doubling behavior and the associated stability of bifurcated solutions of $F\circ G$ also follow immediately from Theorems 3.1 and 3.2.

Example 3.1. Fix $\alpha=0.5$ and $\beta=1$. Consider $G\circ F=G_\eta\circ F_{\alpha,\beta}$, and let η vary in $(0,1)$. We plot the orbit diagram of $G\circ F$, as shown in Fig. 3. According to (51) in Theorem 3.1, the first period-
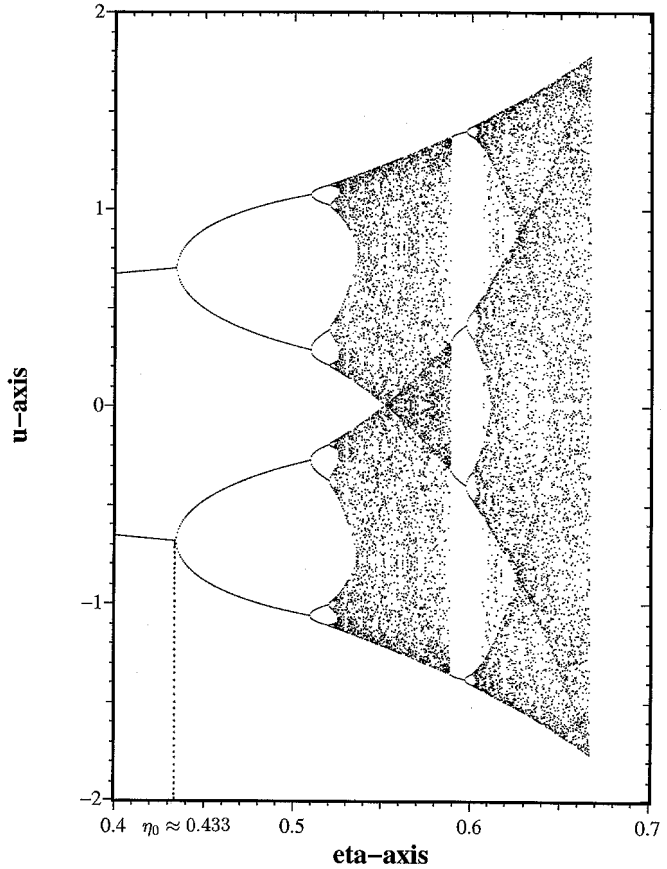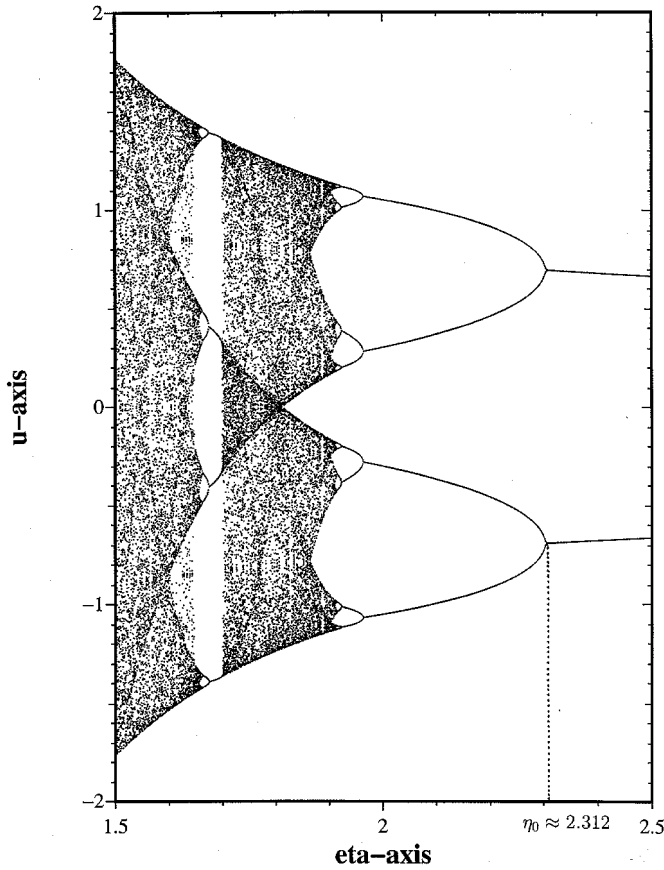

Fig. 3. The orbit diagram of $G_\eta\circ F_{\alpha,\beta}$, where $\alpha=0.5$, $\beta=1$, and η varies in $[0.4, 2/3]$, for Example 3.1. Note that the first period-doubling occurs near $\eta_0\approx 0.433$, agreeing with (61).

doubling should occur at η_0 satisfying

$$\frac{1}{2}\left(\frac{1+0.5\eta_0}{3\eta_0}\right)^{1/2}\left[\frac{1+2\eta_0}{3\eta_0}\right]$$

$$= \frac{1+\eta_0}{2}\sqrt{0.5+\eta_0}, \quad 0<\eta_0<1. \quad (61)$$

The above has a solution $\eta_0 \approx 0.433$, consistent with Fig. 3.

Example 3.2.   Again, fix $\alpha = 0.5$ and $\beta = 1$. Consider $G \circ F = G_\eta \circ F_{\alpha,\beta}$ and let η vary in $(1, \infty)$. We plot the orbit diagram of $G \circ F$ in Fig. 4. According to (60) in Theorem 3.2, the first period-doubling should occur at η_0 satisfying

$$\frac{1}{5}\left(\frac{0.5+\eta_0}{3}\right)^{1/2}(2+\eta_0)$$

$$= \frac{1+\eta_0}{2\eta_0}\sqrt{\frac{1+0.5\eta_0}{\eta_0}}, \quad \eta_0 > 1. \quad (62)$$

It has a solution $\eta_0 \approx 2.312$, consistent with Fig. 4.

Remark 3.2.   Although in the proof of Theorem 3.1, we have taken advantage of the unimodal property of $H = -G \circ F$ for the case of $\eta \in (0, 1)$ to prove the period-doubling of $G \circ F$ itself, we must emphasize that $G \circ F$ is by no means equivalent to a unimodal map. This may be articulated as follows. For a true unimodal map such as the quadratic map $F_\mu(x) = \mu x(1-x)$ on the unit interval, it is well known that its orbit diagram has some "windows" after the completion of period-doubling; see [Devaney, 1989, Fig. 17.7, p. 136], for example, where an attracting period-3 orbit "sucks up most of the chaos". Here in Figs. 3 and 4, we also observe some conspicuous windows. We zoom in Fig. 3 for $\eta \in [0.58, 0.61]$ and display that major window in Fig. 5, where it is clear that an attracting *period-4* orbit has "sucked up most of the chaos for $\eta: 0.5885 \leq \eta \leq 0.5971$. This period-4 seems somehow to defy the period-3-ness in Sharkovsky's

Fig. 4.   The orbit diagram of $G_\eta \circ F_{\alpha,\beta}$, where $\alpha = 0.5$, $\beta = 1$, and η varies in $[1.5, 2.5]$, for Example 3.2. Note that the first period doubling occurs near $\eta_0 \approx 2.312$, agreeing with (62).
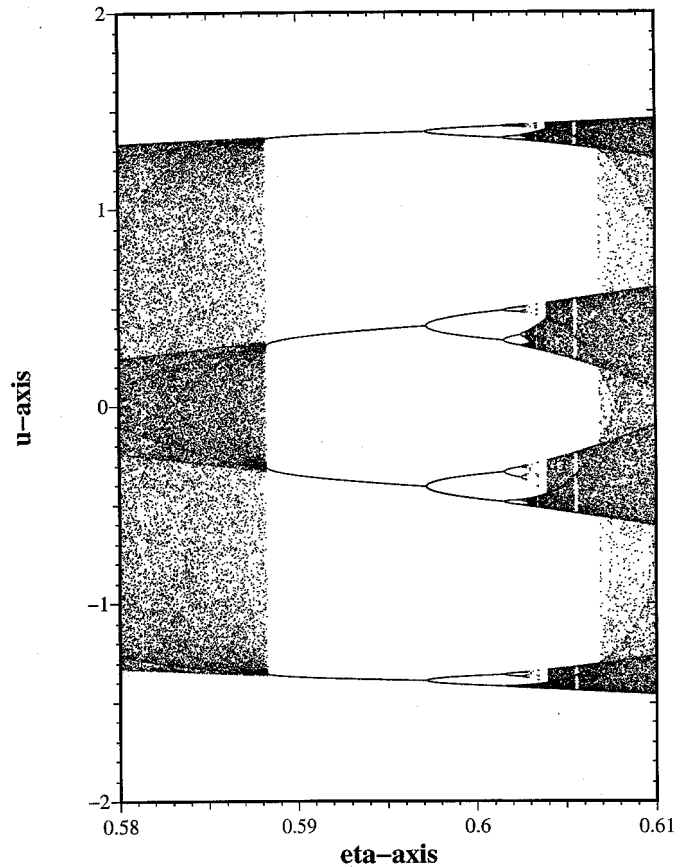

Fig. 5.   Zoom-in of the window in Fig. 3, for $\eta \in [0.58, 0.61]$; see Remark 3.2. Note that a period-4 orbit has sucked up chaos for $0.5885 \leq \eta \leq 0.5971$.
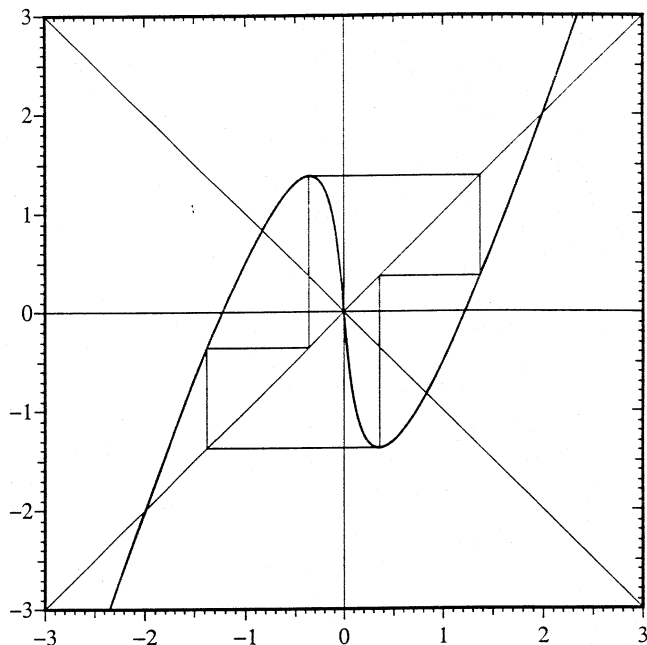
Fig. 6. The globally attracting period-4 orbit referred to in Remark 3.2 and Fig. 5.
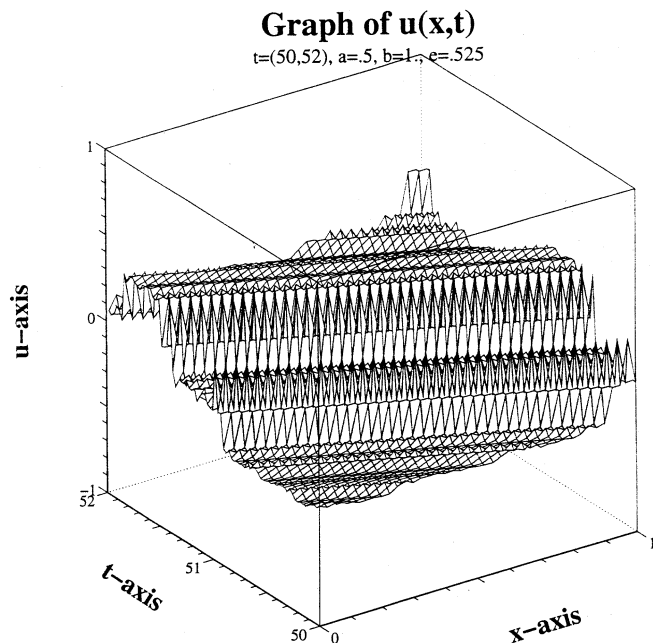
Graph of u(x,t)

t=(50,52), a=.5, b=1, e=.525

Fig. 7. The spatio-temporal profile of the u-component of the system (8)–(11), as given in Example 3.3, for $t \in [50, 52]$, $x \in [0, 1]$, $\alpha = 0.5$, $\beta = 1$, $\eta = 0.525$.
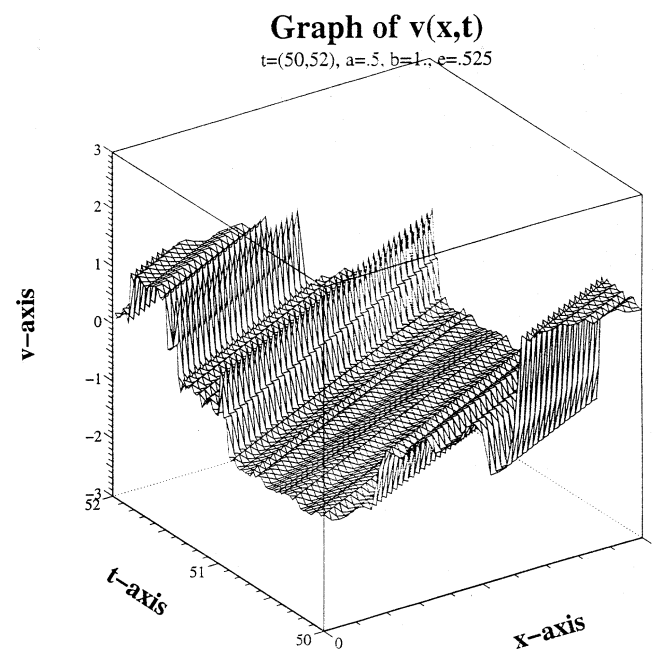
Theorem. Such an attracting period-4 orbit is displayed in Fig. 6. The graph of this orbit is obviously *non-unimodal* in nature.

Example 3.3. We furnish a PDE example. Consider (1)–(4), wherein we set

$$\alpha = 0.5, \quad \beta = 1, \quad \eta = 0.525,$$

$$w_0(x) = 0.2 \sin\left(\frac{\pi}{2}x\right), \qquad (63)$$

$$w_1(x) = 0.2 \sin(\pi x), \qquad x \in [0, 1].$$

Then

$$\left. \begin{array}{l} u_0(x) = 0.1 \left[\dfrac{\pi}{2} \cos\left(\dfrac{\pi}{2}x\right) + \sin(\pi x) \right], \\[3mm] v_0(x) = 0.1 \left[\dfrac{\pi}{2} \cos\left(\dfrac{\pi}{2}x\right) - \sin(\pi x) \right], \end{array} \right\} \; x \in [0, 1].$$

$$(64)$$

For this special choice of $\eta = 0.525$ in (63), the map $G_\eta \circ F_{\alpha,\beta}$ has just completed its period-doubling process, as can be measured from the orbit diagram in Fig. 3. Therefore the solutions u and v of (8)–(11) are both chaotic.

The spatio-temporal profiles of u and v for $0 \leq x \leq 1$, $50 \leq t \leq 52$ are plotted in Figs. 7 and 8. Snapshots for u and v at $t = 52$ are provided in Fig. 9. When $t = 102$, from the snapshots in Fig. 10 we see that even higher frequencies of vibration have appeared.

Graph of v(x,t)
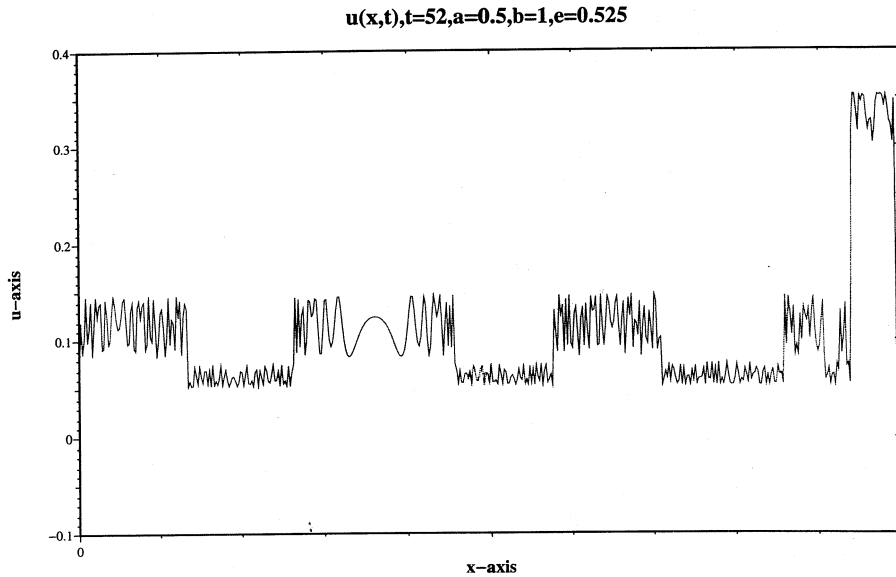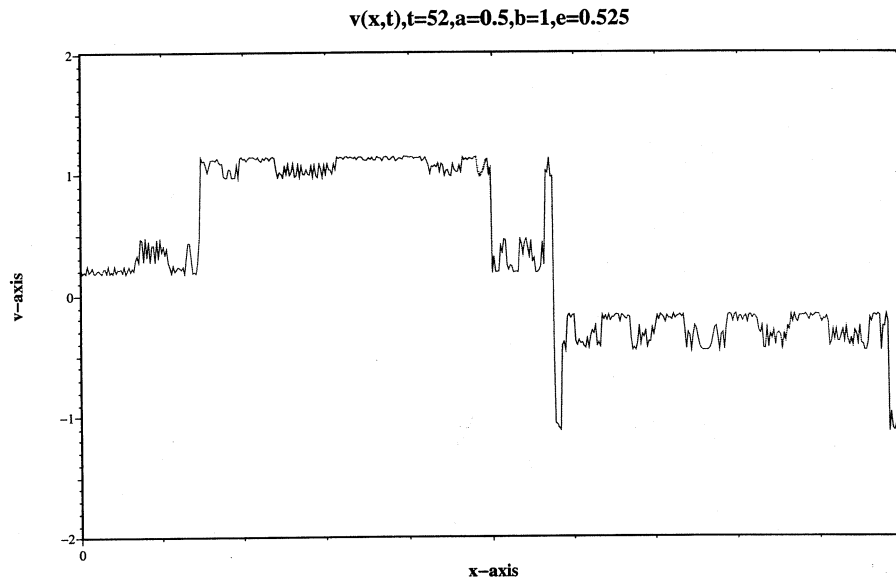
t=(50,52), a=.5, b=1, e=.525

Fig. 8. The spatio-temporal profile of the v-component of the system (8)–(11), as given in Example 3.3, for $t \in [50, 52]$, $x \in [0, 1]$, $\alpha = 0.5$, $\beta = 1$, $\eta = 0.525$.

In our visualization of chaotic vibrations of the wave equation due mainly to period-doubling, we have found that the solution (u, v) seems to somehow manifest a "macroscopically coherent periodic

u(x,t),t=52,a=0.5,b=1,e=0.525

(a)

v(x,t),t=52,a=0.5,b=1,e=0.525

(b)

Fig. 9.   The snapshots of (a) u (b) v, at $t = 52$, for Example 3.3. One may observe some macroscopically coherent periodic pattern. Chaos is visible mainly at a more microscopic scale.

structure". Chaos is visible only at a more micro scale, such as Figs. 9 and 10 have shown.
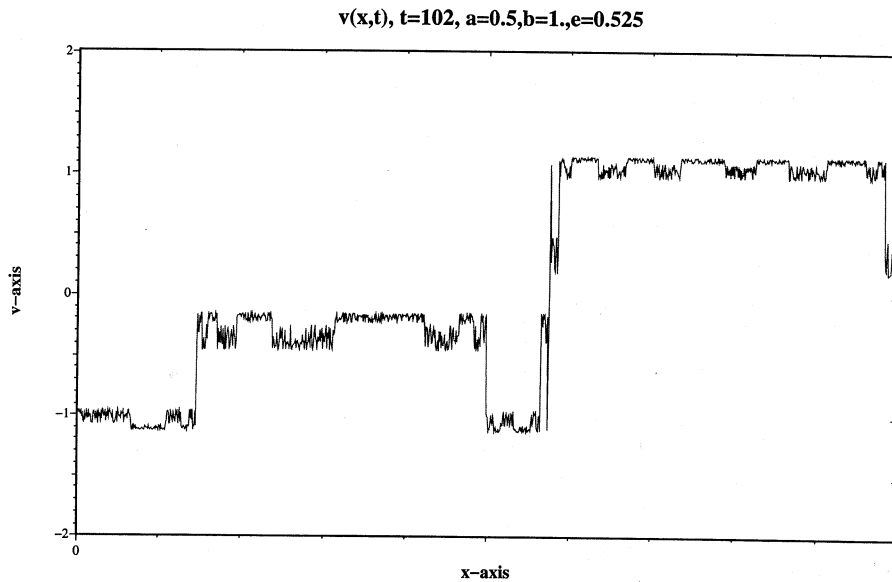
4.   Homoclinic Orbits

Recall the definition of homoclinic points and orbits for a continuously differentiable interval map $f: I \to I$ from [Devaney, 1989, pp. 122–124]. Let p be a repelling fixed point of $f: f(p) = p, |f'(p)| > 1$. Let $W^u_{\text{loc}}(p)$ be the local unstable set at p. A point

$q \in I$ is said to be homoclinic to p if $q \in W^u_{\text{loc}}(p)$ and $f^n(q) = p$ for some $n \in \{1, 2, 3, \ldots\}$. For a homoclinic point q, the set $\{f^j(q)|j = 1, 2, \ldots, n\}$ is said to be the homoclinic orbit of q. The homoclinic orbit of q is said to be *nondegenerate* if $f'(x) \neq 0$ for all points x on the orbit. Otherwise, the homoclinic orbit is said to be *degenerate*.

Theorem 4.1 (Homoclinic Orbits for the Case $0 < \eta < 1$).   *Let $\alpha: 0 < \alpha \leq 1$ and $\beta > 0$ be fixed, and*

u(x,t), t=102, a=0.5,b=1.,e=0.525

(a)

v(x,t), t=102, a=0.5,b=1.,e=0.525
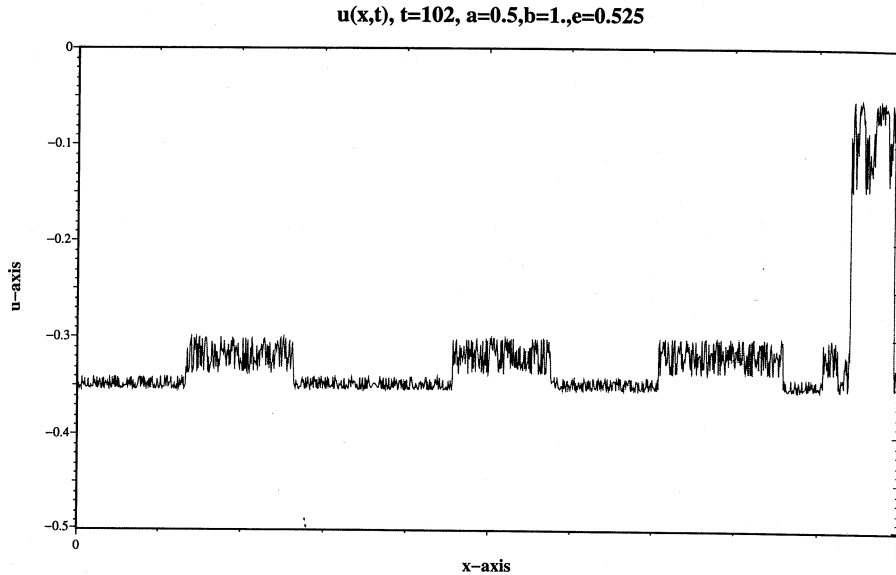
(b)

Fig. 10. The snapshots of (a) u (b) v, at $t = 102$, for Example 3.3. In comparison with Fig. 9, we see that even higher frequencies have appeared.

let $\eta \in (0, 1)$ be a varying parameter. Let $\underline{\eta}_H$ be given by (50). If

$$\underline{\eta}_H \leq \eta < 1 \,, \tag{65}$$

then the repelling fixed point 0 of $G \circ F$ and $F \circ G$ has homoclinic orbits. Furthermore, if $\eta = \underline{\eta}_H$, then there are degenerate homoclinic orbits.

Consequently, if $\eta \in [\underline{\eta}_H, 1)$, then the maps $G \circ F$ and $F \circ G$ are chaotic on some invariant sets of $G \circ F$ and $F \circ G$.

Proof. By (17) and (18), because $g(0) = 0$ we easily get

$$\frac{\partial}{\partial v} f_i(v, \eta)|_{v=0} = \frac{1+\eta}{1-\eta} \left[1 - \frac{2}{1-\alpha} \right]$$

$$= \frac{1+\eta}{1-\eta} \cdot \left(- \left| \frac{1+\alpha}{1-\alpha} \right| \right)$$
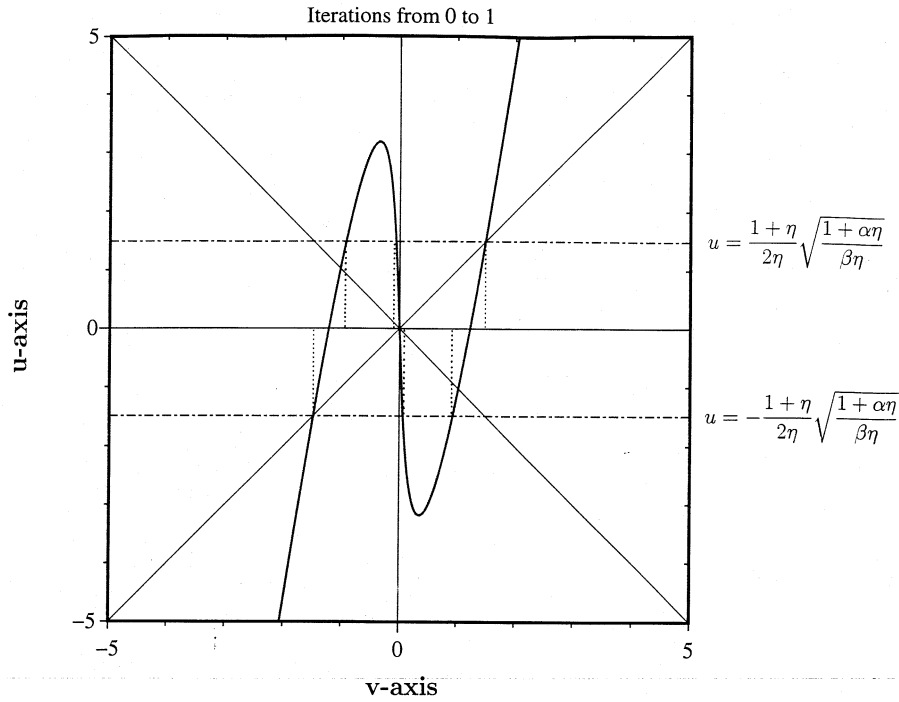
$$< -1 \,, \quad i = 1, 2 \,.$$

Fig. 11. The graph of $G \circ F$, with $\alpha = 0.5$, $\beta = 1$, $\eta = 0.8$. Since the local maximum is larger than the positive v-axis intercept of the graph, we see that homoclinic orbits exist. (Six dotted vertical segments drooped from the curve into the v-axis, making six abscissas $-\tilde{v}_0$, $-\tilde{v}_1$, $-\tilde{v}_2$, $\tilde{v}_2$, $\tilde{v}_1$ and v_0 as given in (74). See Sec. 5.)

Therefore 0 is a repelling fixed point of $G \circ F$ and $F \circ G$. The existence of homoclinic orbits near 0 can be first checked by graphical analysis from Figs. 11 and 12: For a homoclinic orbit to exist, the local maximum of $G \circ F$ (resp., $F \circ G$) must be larger than or equal to the positive v-axis intercept of $G \circ F$ (resp., $F \circ G$). By (32) and (34), we get

$$\frac{1+\eta}{1-\eta}\frac{1+\alpha}{3}\sqrt{\frac{1+\alpha}{3\beta}} \geq \sqrt{\frac{1+\alpha}{\beta}}. \qquad (66)$$

This gives (65) for the map $G \circ F$. For the map $F \circ G$, we use (33) and (38) instead:

$$\frac{1+\alpha}{3}\sqrt{\frac{1+\alpha}{3\beta}} \geq \frac{1-\eta}{1+\eta}\sqrt{\frac{1+\alpha}{\beta}}. \qquad (67)$$

This is exactly the same as (66). We then further check that the backward iterates of the v-axis intercept(s) converge to the origin such that $|f'(x)| > 1$ for each x on this backward orbit. Details are omitted.

When equality holds in (66) and (67), we see that the local maximum is mapped exactly into the repelling fixed point 0. Therefore there exist degenerate homoclinic orbits.

It is well known that chaos occurs when there are homoclinic orbits; see [Devaney, 1989, pp. 124–129]. ■

Theorem 4.2 (Homoclinic Orbits for the Case $\eta > 1$). *Let $\alpha: 0 < \alpha \leq 1$ and $\beta > 0$ be fixed, and let $\eta \in (1, \infty)$ be a varying parameter. Let $\overline{\eta}_H$ be given as in (59). If*

$$\overline{\eta}_H \geq \eta > 1, \qquad (68)$$

then the repelling fixed point 0 of $G \circ F$ and $F \circ G$ has homoclinic orbits. Furthermore, if $\eta = \overline{\eta}_H$, then there are degenerate homoclinic orbits.

Consequently, if $\eta \in (1, \overline{\eta}_H]$, then the maps $G \circ F$ and $F \circ G$ are chaotic on some invariant sets of $G \circ F$ and $F \circ G$.

Proof. The arguments are the same as in the proof of Theorem 4.1. Here, for $G \circ F$, we use (32) and (37):

$$M = -\frac{1+\eta}{1-\eta}\frac{1+\alpha}{3}\sqrt{\frac{1+\alpha}{3\beta}} \geq \sqrt{\frac{1+\alpha}{\beta}}, \qquad (69)$$

which leads to (68). For $F \circ G$, we use (33) and (38):

$$M = \frac{1+\alpha}{3}\sqrt{\frac{1+\alpha}{3\beta}} \geq -\frac{1-\eta}{1+\eta}\sqrt{\frac{1+\alpha}{\beta}},$$

which is equivalent to (69). ■

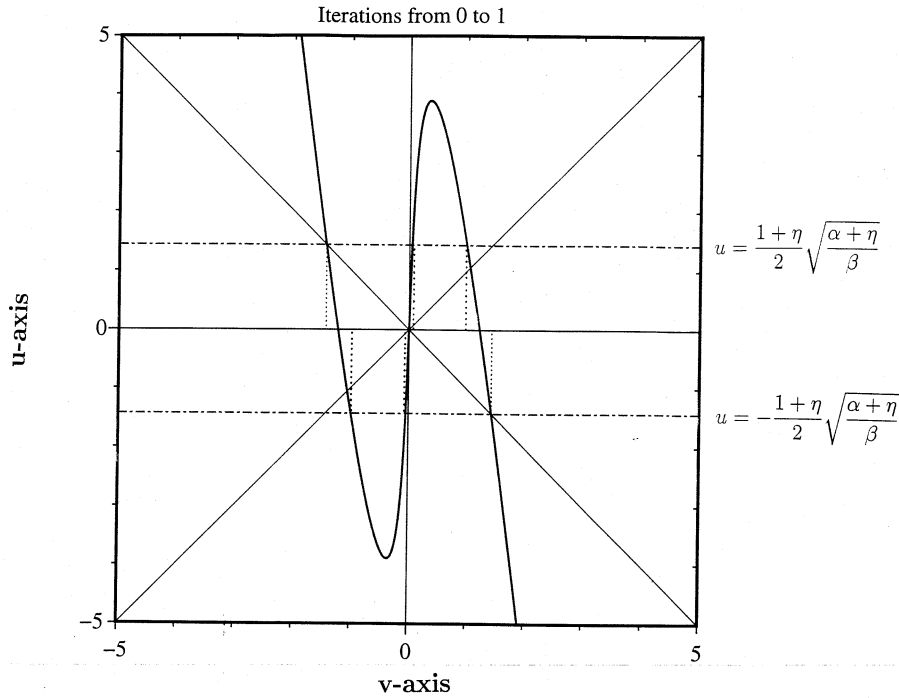Incorporating Lemma 2.5 with Theorems 4.1 and 4.2, we obtain the following two corollaries.

Iterations from 0 to 1

Fig. 12.   The graph of $G \circ F$, with $\alpha = 0.5$, $\beta = 1$, $\eta = 1.2$. Since the local maximum once again is larger than the positive v-axis intercept of the graph, we also have homoclinic orbits. (Also note the six points of intersections of the curve with the horizontal lines $u = \pm[(1 + \eta)/2]\sqrt{(\alpha + \beta)/\beta}$, which are needed in Sec. 5.)

Corollary 4.1. *Let* $0 < \alpha \leq 1$, $\beta > 0$, *and* $\eta \in (0, 1)$. *If* $\underline{\eta}_H \leq \eta \leq \underline{\eta}_B$, *where* $\underline{\eta}_B \in (0, 1)$ *is the unique solution of*

$$\frac{2\underline{\eta}_B}{1 - \underline{\eta}_B}\sqrt{\frac{\underline{\eta}_B}{1 + \alpha\underline{\eta}_B}} = \frac{3\sqrt{3}}{(1 + \alpha)^{3/2}}, \qquad (70)$$

then the maps $G \circ F$ *and* $F \circ G$ *are chaotic on the invariant interval* $\mathcal{I} \equiv [-M, M]$, *where* $M = [(1 + \eta)/(1 - \eta)][(1 + \alpha)/3]\sqrt{(1 + \alpha)/(3\beta)}$.

Proof.   The inequalities (40) and (42) are equivalent, and give

$$\frac{2\eta}{1 - \eta}\sqrt{\frac{\eta}{1 + \alpha\eta}} \leq \frac{3\sqrt{3}}{(1 + \alpha)^{3/2}}. \qquad (71)$$

Note that the LHS of (71) is a strictly increasing function of η for $\eta \in (0, 1)$. Therefore it has a unique solution $\underline{\eta}_B \in (0, 1)$ satisfying (70) after an application of the Intermediate Value Theorem. The rest is obvious from Lemma 2.5 and Theorem 4.1.   ∎

Corollary 4.2. *Let* $0 < \alpha \leq 1$, $\beta > 0$ *and* $\eta > 1$. *If* $\overline{\eta}_B \leq \eta \leq \overline{\eta}_H$, *where* $\overline{\eta}_B \in (1, \infty)$ *is the unique*

solution of

$$(\overline{\eta}_B - 1)\sqrt{\alpha + \overline{\eta}_B} = 2\left(\frac{1 + \alpha}{3}\right)^{3/2}$$

then the maps $G \circ F$ *and* $F \circ G$ *are chaotic on the invariant interval* $\mathcal{I} \equiv [-M, M]$, *where* $M = [(1 + \alpha)/3]\sqrt{(1 + \alpha)/3\beta}$.

Proof.   Same as in the proof of Corollary 4.1. Here, instead, we incorporate Lemma 2.5 (ii) and (iv) with Theorem 4.2.   ∎

The degenerate homoclinic orbits as promised in Theorems 4.1 and 4.2 enable us to establish the existence of an ergodic invariant measure for the map $G \circ F$.

Corollary 4.3. *Let* $\eta^* = \underline{\eta}_H$ *or* $\overline{\eta}_H$ *in Theorems 4.1 and 4.2. Then there exists a set* E *of* η-*values, where* E *has positive Lebesgue measure, such that for all* $\eta \in E$, *the map* $G_\eta \circ F$ *has an absolutely continuous, ergodic, invariant Sinai–Bowen–Ruelle measure (on an invariant set of* $G_\eta \circ F$).

Proof.   We use a theorem due to Benedicks and Carleson [de Melo & van Strien, 1993, Theorem 6.1, p. 403]; we need to verify the Collet–Eckman

condition:

$$\left| \frac{d}{dv} f^i(v) \right|_{v=f(v_c)} \geq CL^i, \quad i = 1, 2, \ldots, \quad (72)$$

is satisfied for $f = h_1(v, \underline{\eta}_H)$ and $f = f_1(v, \overline{\eta}_H)$, respectively, for Theorems 4.1 and 4.2, where v_c (or $\tilde{v}_c$) is the critical point as given in Lemma 2.4, for some $C > 0$, $L > 1$. We have

$$\left. \frac{d}{dv} f^i(v) \right|_{v=f(v_c)} = f'(t_{i-1}) f'(t_{i-2}) \cdots f'(t_0);$$

$$t_j = f^{j+1}(v_c), \quad j = 0, 1, \ldots, i-1.$$

But $t_1 = t_2 = \cdots = t_{i-1} = 0$ because f maps $f(v_c)$ to the fixed point 0. Therefore we get

$$\text{LHS of } (72) = |f'(0)|^{i-1} \cdot |f'(f(v_c))| \geq C(1+\varepsilon)^i,$$
$$\text{for some small } \varepsilon > 0,$$

because $f'(f(v_c)) \neq 0$ (as can be easily verified) and $|f'(0)| > 1$ because the fixed point 0 is repelling.

Therefore, (72) holds with $C \equiv |f'(f(v_c))| / f'(0)| > 0$, $L = 1 + \varepsilon$ for some small $\varepsilon > 0$. ∎

Example 4.1. Let $\alpha = 0.5$, $\beta = 1$. Choose the value $\eta = \underline{\eta}_H$ given in (50):

$$\underline{\eta}_H = \left(1 - \frac{1.5}{3\sqrt{3}} \right) \Big/ \left(1 + \frac{1.5}{3\sqrt{3}} \right) \approx 0.552.$$

The graph of $G \circ F$ has been previously plotted in Fig. 1. The orbits of $G \circ F$ are now displayed in Fig. 13, obtained with 1200 iterations of a few points chosen on the invariant interval $\mathcal{I}$ in Corollary 4.1. Degenerate homoclinic orbits can be easily confirmed. There is very strong chaos due to homoclinic bifurcations, encompassing many period-doubling and saddle-node bifurcations.

Example 4.2. Let $\alpha = 0.5$, $\beta = 1$. Choose $\eta = \overline{\eta}_H$ in (58):

$$\overline{\eta}_H = \left(1 + \frac{1.5}{3\sqrt{3}} \right) \left(1 - \frac{1.5}{3\sqrt{3}} \right)^{-1} \approx 1.812. \quad (73)$$

The orbits of $G \circ F$ on the invariant interval $\mathcal{I}$ in Corollary 4.2 are plotted in Fig. 14. Degenerate homoclinic orbits are again confirmed visually. There is very strong chaos due to homoclinic bifurcations.
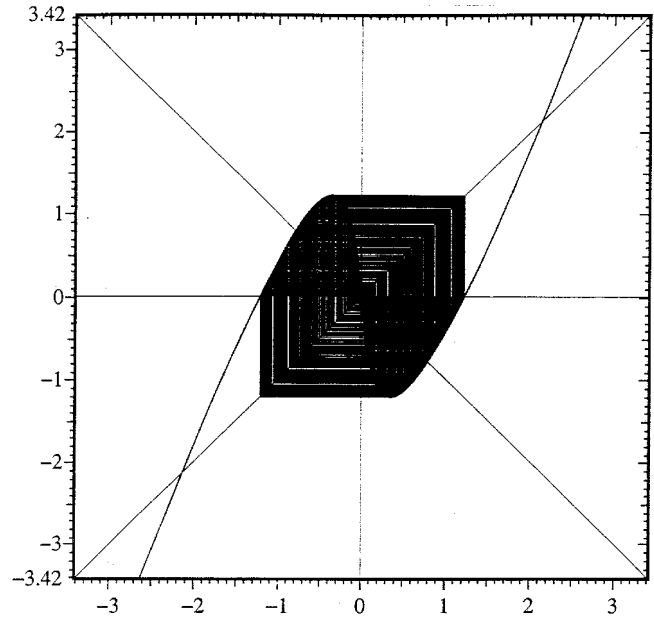

Fig. 13.   "Space-filling" orbits of $G \circ F$, with $\alpha = 0.5$, $\beta = 1$, $\eta = 0.552$ in Example 4.1. Note the presence of degenerate homoclinic orbits and the ensuing strong chaos due to homoclinic bifurcations.
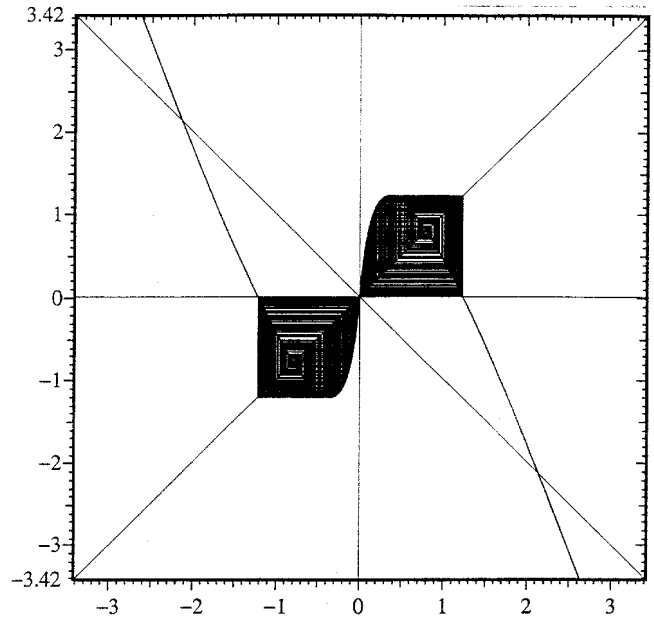

Fig. 14.   "Space-filling" orbits of $G \circ F$, with $\alpha = 0.5$, $\beta = 1$, $\eta = 1.812$ in Example 4.2. Note the presence of degenerate homoclinic orbits and the ensuing strong chaos due to homoclinic bifurcations.

Example 4.3. Consider the very same Example 3.3, with only η in (63) changed to

$$\eta = 1.520.$$

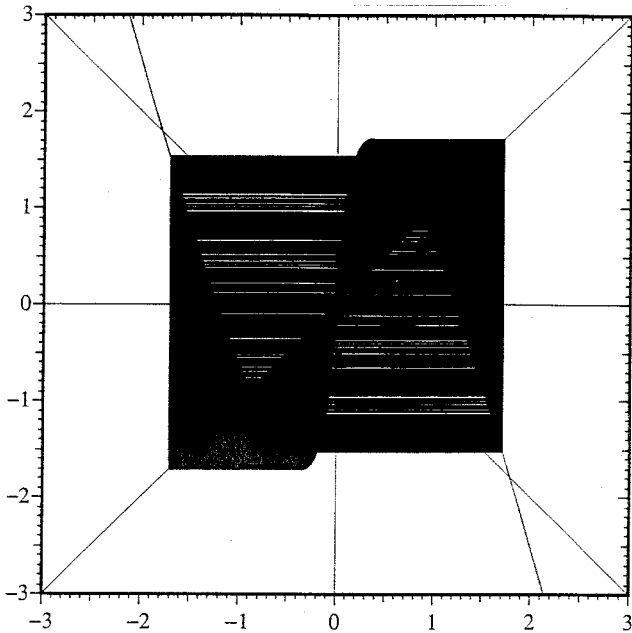It is straightforward to check that (68) is satisfied:

Fig. 15. Orbits of $G \circ F$, with $\alpha = 0.5$, $\beta = 1$, $\eta = 1.520$ in Example 4.3. Note the presence of nondegenerate homoclinic orbits and the ensuing strong chaos.
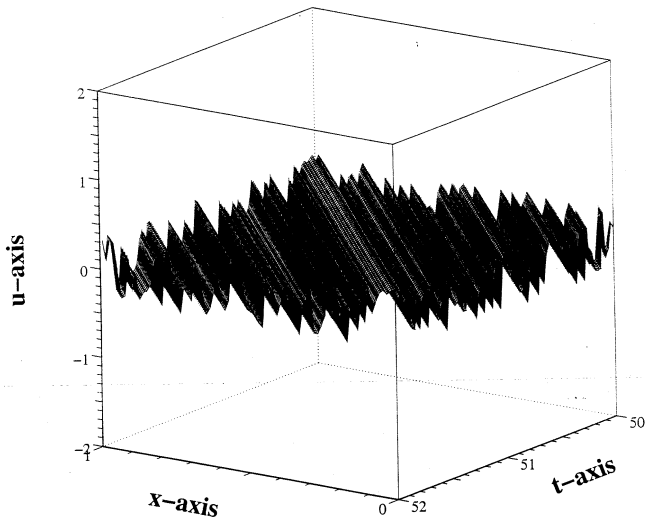

Fig. 16. The spatio-temporal profile of u in Example 4.3, where $\alpha = 0.5$, $\beta = 1$, and $\eta = 1.520$, for $0 \leq x \leq 1$ and $50 \leq t \leq 52$.

$$\overline{\eta}_H = 1.812 > 1.520 > 1. \qquad \text{cf. (73)}$$

Therefore there exists nondegenerate homoclinic orbits of $G \circ F$. This can be easily confirmed in Fig. 15.

The spatio-temporal profiles of u and v are plotted in Figs. 16 and 17, respectively, for $0 \leq x \leq 1$ and $50 \leq t \leq 52$. Snapshots of u and v are given in Fig. 18 at $t = 52$. The profiles look almost like "random white noise". Note that in contrast to
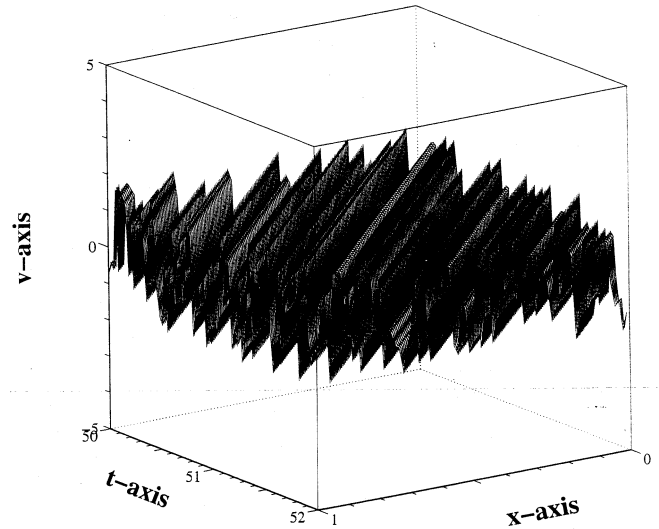

Fig. 17. The spatio-temporal profile of v in Example 4.3, where $\alpha = 0.5$, $\beta = 1$ and $\eta = 1.520$, for $0 \leq x \leq 1$ and $50 \leq t \leq 52$.

Fig. 9, u and v no longer shows any macroscopically coherent periodic structure.

5. Chaos on a Bounded Cantor-like Invariant Subset

When (40) or (41) [equivalently, (42) or (43)] is violated, the maps $G \circ F$ and $F \circ G$ will not have a bounded invariant interval as promised in Lemma 2.5. Consider the case $0 < \eta < 1$ for $G \circ F$, for example. The two horizontal lines $u = \pm[(1 + \eta)/(2\eta)]\sqrt{(1 + \alpha\eta)/(\beta\eta)}$ will intersect the graph of $u = G \circ F(v)$ at a total of six points, as can be seen from Figs. 11 and 12. Two of the six points [see $-\tilde{v}_0$, $\tilde{v}_0$ in (74)] have already been given in (27). We denote the ordered abscissas of these six points by

$$-\tilde{v}_0 \equiv -\frac{1 + \eta}{2\eta}\sqrt{\frac{1 + \alpha\eta}{\beta\eta}}, \ -\tilde{v}_1, \ -\tilde{v}_2, \ \tilde{v}_2, \ \tilde{v}_1, \ \tilde{v}_0,$$
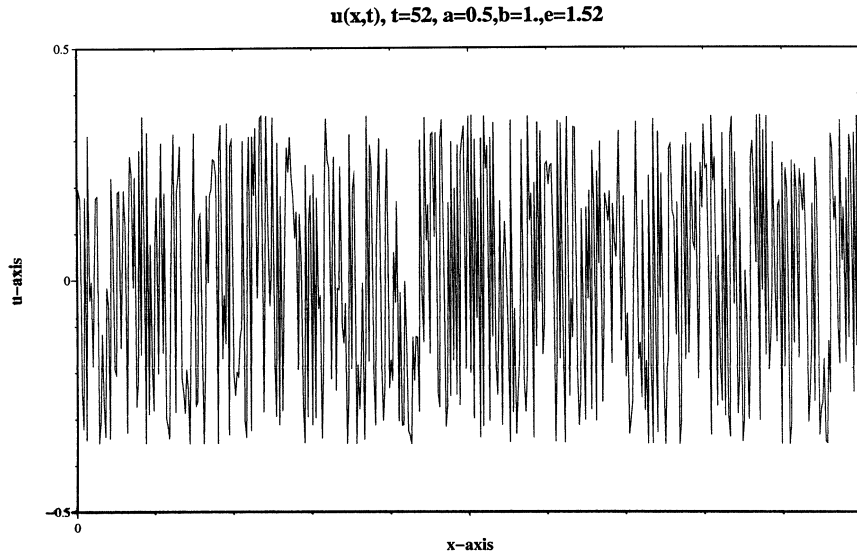
$$(74)$$

where

$$G \circ F(\tilde{v}_1) = G \circ F(\tilde{v}_2) = -\frac{1 + \eta}{2\eta}\sqrt{\frac{1 + \alpha\eta}{\beta\eta}},$$
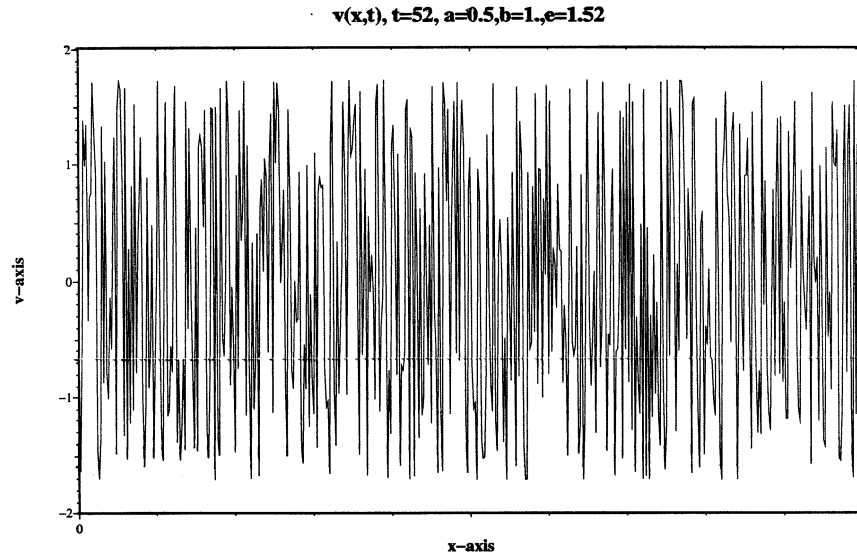
$$(75)$$

$$0 < \tilde{v}_2 < \tilde{v}_1 < \tilde{v}_0 = \frac{1 + \eta}{2\eta}\sqrt{\frac{1 + \alpha\eta}{\beta\eta}}.$$

We then define five intervals

$$I_0 = [-\tilde{v}_0, -\tilde{v}_1], \quad I_1 = [-\tilde{v}_2, \tilde{v}_2], \quad I_2 = -I_0,$$
$$A_0 = (-\tilde{v}_1, -\tilde{v}_2), \quad A_1 = -A_0.$$

$$(76)$$

u(x,t), t=52, a=0.5,b=1.,e=1.52

(a)

v(x,t), t=52, a=0.5,b=1.,e=1.52

(b)

Fig. 18.   The snapshots of (a) u and (b) v, at $t = 52$, for Example 4.3.   In contrast to Fig. 9, macroscopically coherent structures no longer exist.

It is easy to see that

$$v \in \mathcal{I} = [-\tilde{v}_0, \tilde{v}_0], \ (G \circ F)^n(v) \in A_0 \cup A_1$$

$$\text{for some } n \in \{0, 1, 2, \ldots\}$$

$$\Rightarrow \lim_{k \to \infty} |(G \circ F)^k(v)| = \infty. \qquad (77)$$

The set

$$S \equiv \bigcap_{n=0}^{\infty} (G \circ F)^n \mathcal{I} \qquad (78)$$

is a closed bounded invariant subset of the map $G \circ F$. For every point $v \in S$, we can assign an itinerary $s(v)$ of v by

$$s(v) = (s_0 \cdot s_1 s_2 \cdots s_n \cdots)$$

$$s_n = \begin{Bmatrix} 0 \\ 1 \\ 2 \end{Bmatrix} \text{ if } (G \circ F)^n v \in \begin{cases} I_0 \\ I_1 \ , \\ I_2 \end{cases} n = 0, 1, 2, \ldots.$$

$$(79)$$

Then $s(v)$ is a tri-nary number: We have $s(v) \in \sum_3$, where

$$\sum\nolimits_3 = \{s = (s_0 \cdot s_1 s_2 \cdots s_n \cdots)|s_j = 0,\ 1,\ \text{or}\ 2\,,$$

$$j = 0,\ 1,\ 2, \ldots\}\,; \qquad (80)$$

$\sum_3$ is endowed with a natural metric for tri-nary numbers.

We can further make the set S a *hyperbolic repelling set*.

Lemma 5.1. *Let $\alpha: 0 < \alpha \leq 1$ and $\beta > 0$ be given. Then there exists an $\eta_D = \eta_D(\alpha,\ \beta): 0 < \eta_D < 1$ such that if η satisfies $\eta_D < \eta < 1$, then*

$$\left|\frac{\partial}{\partial v} f_1(v,\ \eta)\right| > 1\,, \quad \forall v \in S\,. \qquad (81)$$

Proof. For given α, β, increase η so that

$$\min\left\{\left|\frac{\partial}{\partial v} f_1(v,\ \eta)\right|\ \middle|\ v = \pm \tilde{v}_1,\ \pm \tilde{v}_2\right\} = 1\,. \qquad (82)$$

It can be shown that there exists a unique η_D (depending on α and β) such that (82) holds. We then have

$$\left|\frac{\partial}{\partial v} f_1(v,\ \eta)\right| \geq 1\,, \quad \forall v \in I_0 \cup I_1 \cup I_2\,,\ \eta \geq \eta_D\,,$$

$$\left|\frac{\partial}{\partial v} f_1(v,\ \eta)\right| < 1\,, \quad \forall v \in A_0 \cup A_1\,,\ \eta \geq \eta_D\,.$$

$$(83)$$

(Note that the sets I_0, I_1, I_2, A_0 and A_1 also vary with η.) From (82) and (83), we have

$$\left|\frac{\partial}{\partial v} f_1(v,\ \eta)\right| > 1\,, \quad \forall v \in I_0 \cup I_1 \cup I_2\,,\ \eta > \eta_0\,.$$

Hence (81) holds. ∎

Theorem 5.1. *For given $\alpha: 0 < \alpha \leq 1$ and $\beta > 0$, let η satisfy $\eta_D(\alpha,\ \beta) < \eta < 1$. Then S is a Cantor set with measure zero, and the map $G \circ F$ on S is topologically conjugate to the shift map on $\sum_3$. Consequently, $G \circ F$ is chaotic on S.*

Proof. The method of proof is now standard, see [Devaney, 1989, Sec. 1.7], for example. ∎

Cantor-like bounded invariant sets of $G \circ F$ for the case $\eta > 1$, and of $F \circ G$ for both $0 < \eta < 1$ and $\eta > 1$ cases, can be similarly constructed whereupon $G \circ F$ and $F \circ G$ are topologically conjugate to a shift map. We omit the details.

6. Differentiable Solutions

All except the trivial solution $(u(x,\ t),\ v(x,\ t)) \equiv (0,\ 0)$ proven to be chaotic in Parts I and III [Chen *et al.*, 1998, 1998] are *discontinuous* solutions on the space-time domain $\{(x,\ t)|0 < x < 1,\ t > 0\}$. However, for the problem which we are treating in this paper, the solutions $(u,\ v)$ and w can have *arbitrarily high order of differentiability*, provided that the initial conditions are smooth and certain compatibility conditions are met.

To examine the questions of continuity and differentiability of the solutions w and $(u,\ v)$, we are first reminded that discontinuities of w and $(u,\ v)$, as solutions of hyperbolic PDEs, can only propagate along characteristics [Courant & Hilbert, 1962, Sec. V.1]. This fact is well reflected in the representation formulas for $(u,\ v)$ given in (13) and (14). The "fault lines", where the representation formulas for u and v switch from one region to another, have six possibilities as indicated on the right half of (13) and (14). Substituting $\tau = t - 2k$ therein and changing inequality to equality, we get

$$t - 2k = 1 - x\,, \quad t - 2k = 2 - x\,,$$
$$t - 2k = 2\,, \qquad (84)$$

$$t - 2k = x\,,\ t - 2k = 1 + x\,,\ t - 2k = 2\,. \quad (85)$$

The two horizontal line segments $t - 2k = 2$ on the rightmost of (84) and (85) should be excluded because they are not really the characteristic lines of discontinuities. Therefore, simplifying the rest of (84) and (85), we get four families of line segments along which discontinuities may propagate:

$$x + t = 2k\,, \quad x + t = 2k + 1\,, \quad t - x = 2k\,,$$
$$t - x = 2k + 1\,,\ \text{for}\ 0 \leq x \leq 1,\ t \geq 0,\ k \in \mathbb{Z}^+\,.$$
$$(86)$$

Theorem 6.1. *Let $(u,\ v)$ be the solution of the system (8)–(11) in the sense of method of characteristics as represented by (13) and (14). Assume that the initial conditions u_0, $v_0 \in C^m([0,\ 1])$ for some $m \in \mathbb{Z}^+$. In addition, assume that at the left end $x = 0$, we have*

$$v_0^{(k)}(0) = (-1)^k \cdot \frac{1 + \eta}{1 - \eta} u_0^{(k)}(0)\,, \quad k = 0,\ 1, \ldots,\ m\,.$$
$$(87)$$

Also at the right end $x = 1$, assume that we have

$$u_0^{(k)}(1) = (-1)^k \cdot \mathcal{F}_k(F, F', \ldots, F^{(k)}, v_0(1), \quad v_0'(1), \ldots, v_0^{(k)}(1)), \quad k = 0, 1, \ldots, m, \tag{88}$$

where

$$
\begin{aligned}
\mathcal{F}_0 &= F(v_0(1)), \qquad \mathcal{F}_1 = F'(v_0(1))v_0'(1), \\
\mathcal{F}_2 &= F''(v_0(1))v_0'(1)^2 + F'(v_0(1))v_0''(1), \\
\mathcal{F}_3 &= F'''(v_0(1))[v_0'(1)]^3 + 3F''(v_0(1))v_0''(1)v_0'(1) + F'(v_0(1))v_0'''(1), \\
&\cdots \\
\mathcal{F}_m &= F^{(m)}(v_0(1))[v_0'(1)]^m + \cdots + F'(v_0(1))v_0^{(m)}(1).
\end{aligned}
\tag{89}
$$

Then the solution (u, v) is C^m-continuous on the space-time domain $[0, 1] \times [0, T]$ for any $T > 0$.

Proof. Let $\vec{a} = (a_1, a_2) \in \mathbb{R}^2$ be any unit vector on the (x, t)-plane, and let $D_{\vec{a}}$ be the directional derivative along $\vec{a}$. We want to show that $(D_{\vec{a}})^j u$ and $(D_{\vec{a}})^j v$ are continuous across the characteristics line segments in (86), for $j = 0, 1, \ldots, m$, for any $k \in \mathbb{Z}^+$.

Take $(14)_1$ and $(14)_2$ across the characteristics $t - x = 2k$, for example:

$$
v(x, t) = \begin{cases}
(G \circ F)^k(v_0(x - \tau)) = (G \circ F)^k(v_0(x - t + 2k)), & t - 2k \le x \le 1, \\
G \circ (F \circ G)^k(u_0(\tau - x)) = (G \circ F)^k \left(\dfrac{1+\eta}{1-\eta} u_0(t - x - 2k) \right), & x < t - 2k \le 1 + x.
\end{cases}
$$

To have $v(x, t)$ C^m-continuous across $t - x = 2k$, we must have

$$D_{\vec{a}}^j[(G \circ F)^k(v_0(x-t+2k))]|_{x-t+2k=0}$$

$$= D_{\vec{a}}^j \left[(G \circ F)^k \left(\frac{1+\eta}{1-\eta} u_0(t-x-2k) \right) \right] \Bigg|_{x-t+2k=0},$$

$$j = 0, 1, 2, \ldots, m.$$

This is easily seen to lead to (87).

Similarly, using $(13)_{1,2}$ and comparing their $D_{\vec{a}}^j$ along $x + t = 2k + 1$ for $j = 0, 1, 2, \ldots, m$, we get (89).

All the other cases also lead to the same compatibility conditions (87) and (89). We omit the details. ∎

Corollary 6.1. *Let w be the solution of (1)–(4) such that the initial conditions (w_0, w_1) satisfy $w_0 \in C^{m+1}([0, 1])$ and $w_1 \in C^m([0, 1])$, for some non-negative integer m. Let (u_0, v_0) be defined as in (11), and satisfy (87)–(89). Then w is C^{m+1}-continuous on $[0, 1] \times [0, T]$ for any $T > 0$.*

Example 6.1. Let $w_0, w_1 \in C^\infty([0, 1])$. Furthermore, $w_0^{(j)}(0) = w_1^{(j)}(0) = w_0^{(j)}(1) = w_1^{(j)}(1) = 0$, for all $j \in \mathbb{Z}^+$. Then the solution w of (1)–(4) is

C^∞-continuous on $[0, 1] \times [0, T]$ for any $T > 0$.

Let w be a C^{m+1}-continuous solution of (1)–(4) for some $m \ge 1$, and let $W(x, t) = w_t(x, t)$. Then W again satisfies the wave equation

$$W_{tt}(x, t) - W_{xx}(x, t) = 0, \quad 0 < x < 1, \ t > 0, \tag{90}$$

as well as the linear boundary condition at the left end $x = 0$:

$$W_t(0, t) = -\eta W_x(0, t), \quad \eta > 0, \ \eta \ne 1, \ t > 0. \tag{91}$$

The initial conditions now become

$$
\begin{aligned}
W(x, 0) &= w_1(x) \in C^m([0, 1]), \\
W_t(x, 0) &= w_{tt}(x, 0) = w_{xx}(x, 0) \tag{92} \\
&= w_0''(x) \in C^{m-1}([0, 1]).
\end{aligned}
$$

How about the right end boundary condition? Differentiating (2) with respect to t, we get

$$w_{xt}(1, t) = \alpha w_{tt}(1, t) - 3\beta w_t^2(1, t)w_{tt}(1, t),$$

or

$$W_x(1, t) = [\alpha - 3\beta W^2(1, t)]W_t(1, t), \quad t > 0. \tag{93}$$

Note that the boundary condition (93) is also a self-excitation boundary condition, analogous to the van der Pol ODE

$$\ddot{x} + (-\alpha + 3\beta x^2)\dot{x} + \omega_0^2 x = 0\,,$$

which we have mentioned in Part I [Chen *et al.*, 1998a] but have not been able to treat it by directly applying the method of characteristics.

Theorem 6.2. *Let* w *and* $(u,\, v)$ *be, respectively, the solutions of the hyperbolic PDEs given in Corollary 6.1 and Theorem 6.1, with* $m \geq 1$ *therein. Let* $W(x,\, t) = w_t(x,\, t)$. *Assume that* $\alpha \colon 0 < \alpha \leq 1$, $\beta > 0$ *and* $\eta > 0$, $\eta \neq 1$ *are given such that according to Secs. 3–Sec. 5,* u *and* v *are chaotic. Then* W *is the unique solution of* (90)–(93), W *is* C^m-*continuous on* $[0,\, 1] \times [0,\, T]$ *for any* $T > 0$, *and* W *is* (*generically*) *chaotic.*

Proof: Since $W(x,\, t) = w_t(x,\, t)$, using the topological conjugacy in Part I [Chen *et al.*, 1998, Sec. 5], we immediately see that W is chaotic. The rest is obvious. ∎

Theorem 6.2 tells us that it is possible to have smooth, unique solutions of the system (90)–(93), whose *trajectory* (or *state*) W itself is chaotic, with the boundary condition (93) which is much harder to treat than (2). In our other work [Chen *et al.*, 1996, 1998, 1998], chaos has been shown to exist only at the $(u,\, v)$ or the gradient $(w_x,\, w_t)$ level.

Acknowledgments

References

Chen, G., Hsu, S. B. & Zhou, J. [1996] "Linear superposition of chaotic and orderly vibrations on two serially connected strings with a van der Pol joint," *Int. J. Bifurcation and Chaos* **6**, 1509–1527.

Chen, G., Hsu, S. B. & Zhou, J. [1998a] "Chaotic vibrations of the one-dimensional wave equation due to a self-excitation boundary condition, Part I: Controlled hysteresis," *Trans. Amer. Math. Soc.*, to appear.

Chen, G., Hsu, S. B. & Zhou, J. [1998b] "Chaotic vibrations of the one-dimensional wave equation due to a self-excitation boundary condition. III. Natural hysteresis memory effects," *Int. J. Bifurcation and Chaos* **8**(3), 447–470.

Chen, G. & Zhou, J. [1993] *Vibration and Damping in Distributed Systems, Vol. I: Analysis, Estimation, Attenuation and Design* (CRC Press, Boca Raton, FL), p. 24.

Chen, G. R. & Lai, D. J. [1997] "Making a dynamical system chaotic: Feedback control of Lyapunov exponents for discrete time dynamical systems," *IEEE Trans. Circuits Syst.*-I **44**, 250–253.

Chow, S. N. & Hale, J. K. [1982] *Methods of Bifurcation Theory* (Springer, New York).

Collet, C. & Tresser, C. [1978] "Itération d'endomorphismes et de groupe de renormalisation," *J. de Physique Colloque* **39**, C5–C25.

Courant, R. & Hilbert, D. [1962] *Methods of Mathematical Physics*, Vol. II (Wiley-Interscience, New York).

de Melo, W. & van Strien, S. [1993] *One Dimensional Dynamics* (Springer-Verlag, New York).

Devaney, R. L. [1989] *An Introduction to Chaotic Dynamical Systems* (Addison-Wesley, New York).

Feigenbaum, M. [1978] "Quantitative universality for a class of non-linear transformations," *J. Stat. Phys.* **21**, 25–52.

Robinson, C. [1995] *Dynamical Systems, Stability, Symbolic Dynamics and Chaos* (CRC Press, Boca Raton, FL).

Sharkovsky, A. N. [1994] "Ideal turbulences in an idealized time-delayed Chua's circuit," *Int. J. Bifurcation and Chaos* **4**(2), 303–309.

Shimura, M. [1967] "Analysis of some nonlinear phenomena in a transmission line," *IEEE Trans. Circuit Theor.* **14**, 60–69.